Syntheses, Structures, Some Reactions, and Electrochemical Oxidation of Ferrocenylethynyl Complexes of Iron, Ruthenium, and Osmium

Michael I. Bruce,*[,†] Paul J. Low,*[,‡] František Hartl,[§] Paul A. Humphrey,[†] Frédéric de Montigny,[†,||] Martyn Jevric,[†] Claude Lapinte,[||] Gary J. Perkins,[†] Rachel L. Roberts,[‡] Brian W. Skelton,[⊥] and Allan H. White[⊥]

Department of Chemistry, University of Adelaide, South Australia 5005, Department of Chemistry, University of Durham, South Road, Durham DH1 3LE, England, Van't Hoff Institute for Molecular Sciences, University of Amsterdam, Nieuwe Achtergracht 166, 1018 WV Amsterdam, The Netherlands, UMR CNRS 6509, Institut de Chimie, Campus de Beaulieu, Université de Rennes 1, 35042 Rennes, France, and Chemistry M313, School of Biomedical, Biomolecular and Chemical Sciences, University of Western Australia, Crawley, Western Australia 6009

Received June 11, 2005

The syntheses and characterizations of several complexes containing ferrocenylethynyl and ferrocene-1,1′-bis(ethynyl) groups attached to M(PP)Cp′ [M = Fe, Ru, PP = dppe, Cp′ = Cp*; M = Ru, Os, PP = $(PPh_3)_2$, dppe, Cp′ = Cp] are described. Reactions with tetracyanoethene have given either tetracyanobuta-1,3-dienyl or η^3-allylic derivatives, while addition of Me^+ afforded the corresponding vinylidene derivatives. Some electrochemical measurements are discussed in terms of electronic communication between the redox-active M(PP)Cp′ groups through the ferrocene nucleus. The molecular structures of 14 of these complexes have been determined by crystallographic methods.

Introduction

Complexes containing carbon chains end-capped by various transition metal−ligand combinations have been proposed as models for molecular wires.[1] In this context, interest centers on those compounds that contain carbon chains end-capped by redox-active metal centers, among which the $MnX(dmpe)_2$,[2] $Re(NO)(PPh_3)Cp^*$,[3] $Fe(CO)_2Cp^*$,[4] Fe(dppe)Cp*,[5] and Ru(PP)Cp′ [Cp′ = Cp, PP = $(PPh_3)_2$; Cp′ = Cp*, PP = dppe][6] (dppe = 1,2-bis(diphenylphosphino)ethane, $PPh_2CH_2CH_2PPh_2$) systems have been most studied. Attention has also been focused on complexes containing ferrocenyl groups, and we have earlier published a study of complexes $Fc(C{\equiv}C)_nW(CO)_3Cp$ (n = 1−4) (Fc = ferrocenyl, $Fe(\eta\text{-}C_5H_4-)Cp$) in which we showed that lengthening of the carbon chain from two to eight carbons resulted in an increase in oxidation potential of the ferrocenyl moiety.[7] This is consistent with both a gradual increase in the degree of electron transfer from the Fc nucleus to the chain and the decreased σ-donor ability of the longer carbon chains, i.e., the higher acidity of poly-ynes vs acetylenes.

End-capping of carbon chains with both Fc and another redox-active group, such as those mentioned above, has been reported previously in the systems McC≡CRu(PP)Cp′ [Mc = Fc, Rc; PP = $(PPh_3)_2$ (**1**), dppe (**2**), dppf; Cp′ = Cp, Cp*[8] (dppf = 1,1-bis(diphenylphosphino)ferrocene, $Fe(\eta\text{-}C_5H_4PPh_2)_2$; Rc = ruthenocenyl, $Ru(\eta\text{-}C_5H_4-)Cp$)]. Electrochemical and spectroscopic studies showed that there is a considerable electronic interaction between the two end-caps mediated by the carbon chain, so that the radical cation derived from one-electron oxidation displays some delocalized character. To date, no examples of ferrocene derivatives

* To whom correspondence should be addressed. Tel: +44 (0)191 334 2114. Fax: +44 (0)191 384 4737. E-mail: p.j.low@durham.ac.uk.
† University of Adelaide.
‡ University of Durham.
§ University of Amsterdam.
|| Université de Rennes 1.
⊥ University of Western Australia.

(1) Bruce, M. I.; Low, P. J. *Adv. Organomet. Chem.* **2004**, *50*, 231.
(2) Fernandez, F. J.; Venkatesan, K.; Blacque, O.; Alfonso, M.; Schmalle, H. W.; Berke, H. *Chem. Eur. J.* **2003**, *9*, 6192.
(3) (a) Brady, M.; Weng, W.; Zhou, Y.; Seyler, J. W.; Amoroso, A. J.; Arif, A. M.; Bohme, M.; Frenking, G.; Gladysz, J. A. *J. Am. Chem. Soc.* **1997**, *119*, 775. (b) Bartik, T.; Weng, W.; Ramsden, J. A.; Szafewrt, S.; Falloon, S. B.; Arif, A. M.; Gladysz, J. A. *J. Am. Chem. Soc.* **1998**, *120*, 11071. (c) Dembinski, R.; Bartik, T.; Bartik, B.; Jaeger, M.; Gladysz, J. A. *J. Am. Chem. Soc.* **2000**, *122*, 810.
(4) (a) Akita, M.; Moro-oka, Y. *Bull. Chem. Soc. Jpn.* **1995**, *68*, 420. (b) Akita, M.; Chung, M.-C.; Sakurai, A.; Sugimoto, S.; Terada, M.; Tanaka, M.; Moro-oka, Y. *Organometallics* **1997**, *16*, 4882. (c) Sakurai, A.; Akita, M.; Moro-oka, Y. *Organometallics* **1999**, *18*, 3241. (d) Akita, M.; Sakurai, A.; Chung, M.-C.; Moro-oka, Y. *J. Organomet. Chem.* **2003**, *670*, 2.
(5) Le Narvor, N.; Toupet, L.; Lapinte, C. *J. Am. Chem. Soc.* **1995**, *117*, 7129. (b) Coat, F.; Guillevic, M.-A.; Toupet, L.; Paul, F.; Lapinte, C. *Organometallics* **1997**, *16*, 5988. (c) Guillemot, M.; Toupet, L.; Lapinte, C. *Organometallics* **1998**, *17*, 1929. (d) Coat, F.; Paul, F.; Lapinte, C.; Toupet, L.; Costuas, K.; Halet, J.-F. *J. Organomet. Chem.* **2003**, *683*, 368.
(6) (a) Bruce, M. I.; Low, P. J.; Costuas, K.; Halet, J.-F.; Best, S. P.; Heath, G. A. *J. Am. Chem. Soc.* **2000**, *122*, 1949. (b) Bruce, M. I.; Kelly, B. D.; Skelton, B. W.; White, A. H. *J. Organomet. Chem.* **2000**, *604*, 150. (c) Bruce, M. I.; Ellis, B. G.; Low, P. J.; Skelton, B. W.; White, A. H. *Organometallics* **2003**, *22*, 3184.
(7) Bruce, M. I.; Smith, M. E.; Skelton, B. W.; White, A. H. *J. Organomet. Chem.* **2001**, *637−639*, 484.
(8) (a) Sato, M.; Shintate, H.; Kawata, Y.; Sekino, M.; Katada, M.; Kawata, S. *Organometallics* **1994**, *13*, 1956. (b) Sato, M.; Hayashi, Y.; Kumakura, S.; Shimizu, N.; Katada, M.; Kawata, S. *Organometallics* **1996**, *15*, 721. (c) Sato, M.; Kawata, Y.; Shintate, H.; Habata, Y.; Akabori, S.; Unoura, K. *Organometallics* **1997**, *16*, 1693.

10.1021/om050483l CCC: $30.25
Publication on Web 09/23/2005

Scheme 1

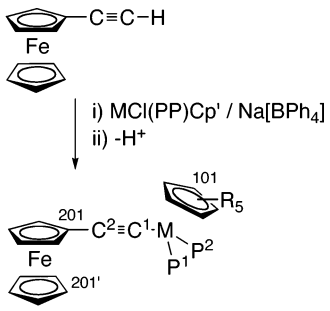

	M	PP	R
1-Ru	Ru	$(PPh_3)_2$	H
1-Os	Os	$(PPh_3)_2$	H
2	Ru	dppm	H
3-Ru	Ru	dppe	H
3-Os	Os	dppe	H
4	Ru	dppe	Me

containing two metal-ethynyl substituents have been reported, and this paper reports on the use of the 1,1′-ferrocenediyl unit (Fc′; ferrocene-1,1′-diyl, Fe(η-C_5H_4-)$_2$) as a bridge between two redox-active metal centers. Also described are derivatives of these alkynyl compounds formed by adding electrophiles, such as the electron-deficient alkene tetracyanoethene (tcne) and Me^+, to the C≡C triple bond.

Results and Discussion

A modified synthesis of Ru(C≡CFc)(PP)Cp′ [Cp′ = Cp, PP = $(PPh_3)_2$ (**1-Ru**), dppm (**2**), dppe (**3-Ru**); Cp = Cp*, PP = dppe (**4**)] was used, whereby a mixture of RuCl(PP)Cp′, FcC≡CH, and Na[BPh_4] was heated in refluxing methanol, followed by addition of sodium methoxide solution; for the synthesis of **2**, thf−NEt_3 (1/1) was used to improve solubility with the amine also serving as a base to deprotonate the vinylidene intermediate (Scheme 1). The osmium analogues of **1-Ru** (**1-Os**) and **3-Ru** (**3-Os**) were prepared and characterized similarly, the reactions requiring 2 h heating. The complexes were obtained in 55−82% yields. While **1**, **3-Ru**, and **4** have all been described previously,[8] identification of all complexes described herein has followed from their spectroscopic properties (IR, NMR, ES mass), and the structures of most were confirmed by X-ray determinations. Correct elemental microanalyses were obtained for all complexes described herein. In solution the IR spectra contain ν(C≡C) bands at ca. 2080 cm^{-1}. The NMR data for the known complexes agreed with the previously reported values. In general, Cp resonances were found at δ_H ca. 4.0 (FeCp) and 4.8 (RuCp) and δ_C ca. 66−69 (FeCp), 80−86 (RuCp), and 78.6 (OsCp) (Table 1). The substituted C_5H_4 groups of the ferrocene moieties gave unresolved multiplets between δ_H 3.75 and 3.8 and two unresolved multiplets at δ_C ca. 66.5 and ca. 70.7; the *ipso* carbons of the ferrocenes were at δ ca. 77−78. Resonances for the Ph groups of the phosphine ligands and for the CH_2 fragments of dppm and dppe were located in the normal ranges, although the large downfield shift of the ^{31}P signal for the coordinated PPh_3 ligand, from δ 51.87 (**1-Ru**) to 2.93 (**1-Os**), is of note. The acetylenic carbons (Table 2) appear between δ_C 105−120 (Ru−C_α), 82−82 (Os−C_α), and 104−109 (C_β), with C_α showing a triplet J(CP) coupling to the two ^{31}P nuclei of the supporting phosphine ligand(s).

As the compound 1,1′-$(HC{\equiv}C)_2$Fc′ is rather unstable,[9] a general approach to the synthesis of the disubstituted ferrocenes was developed using the metallo-desilylation reaction of alkynyltrimethylsilanes described earlier.[10] Thus, reactions of 1,1′-$(Me_3SiC{\equiv}C)_2$Fc′ with ruthenium complexes RuCl(PP)Cp′ in MeOH or MeOH−thf mixtures in the presence of KF afforded 50−60% yields of the corresponding complexes 1,1′-{Cp′(PP)RuC≡C}$_2$Fc′ [Cp′ = Cp, PP = $(PPh_3)_2$ (**5**), dppe (**6**); Cp′ = Cp*, PP = dppe (**7**)] (Scheme 2). The analogous iron complex, 1,1′-{Cp*(dppe)FeC≡C}$_2$Fc′ (**8**), was also prepared and isolated as orange crystals in 60% yield by a similar reaction from FeCl(dppe)Cp*. These trimetallic complexes were identified by spectroscopic methods and by X-ray structural determinations of **5**, **7**, and **8**. A byproduct identified as 1-($Me_3SiC{\equiv}C$)-1′-{Cp(dppe)-RuC≡C}Fc′ (**9**) was obtained in 11% yield from the reaction that afforded **6**, and the Cp* analogue **10** was made directly (46% yield) by using half an equivalent of RuCl(dppe)Cp* in a similar reaction.

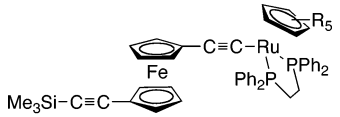

R = H (**9**), Me (**10**)

For complexes **5**−**8**, the ν(C≡C) bands are found between 2065 and 2080 cm^{-1} in their IR spectra. Singlet RuCp resonances occur between δ_H 4.45 and 4.72, with C_5H_4 protons from the ferrocenyl residues between δ_H 3.57 and 4.58: the latter move to higher frequency with the more electron-rich ruthenium groups. The spectra of the Cp* complexes **7**, **8**, and **10** contain the ring Me resonances at δ_H 1.63−1.68. The $SiMe_3$ groups in **9** and **10** resonated at δ_H 0.23 and 0.27, respectively. Only **10** proved soluble enough to obtain satisfactory ^{13}C NMR spectra, in which resonances appeared at δ 10.76 and 92.97 (Cp* Me and ring carbons), between 29.9 and 30.5, and 127−140 (dppe CH_2 and Ph), and at δ 69.8, 65.2 and 73.4, and 79.0 (Fe−Cp, C_α, C_β, and C_{ipso} of Fe−C_5H_4). In all of the trimetallic complexes, ^{31}P resonances occur in characteristic regions, at δ_P ca. 52 for PPh_3 and 80−85 (dppe), while in the ES mass spectra, isotopic envelopes corresponding to M^+ or $[M + nH]^{n+}$ ions were observed.

Although **5** proved to be relatively insoluble in common solvents, the more soluble mono-oxidized species [**5**]PF_6 was readily obtained by reaction of **5** with [$FeCp_2$]-PF_6 in a dichloromethane−benzene mixture. The authenticity of [**5**]PF_6 was confirmed by microanalysis. The IR spectrum of [**5**]PF_6 as a Nujol mull contained strong ν(CC) and ν(PF) absorptions at 1993 and 841 cm^{-1}, respectively, with the decrease in frequency of the ν(CC) band relative to that in neutral **5** [ν(CC) 2101, 2069 cm^{-1}] suggesting some change in the Ru−C−C−Fc

(9) Doisneau, G.; Balavoine, G.; Fillebeen-Khan, T. *J. Organomet. Chem.* **1992**, *425*, 113.

(10) Bruce, M. I.; Hall, B. C.; Kelly, B. D.; Low, P. J.; Skelton, B. W.; White, A. H. *J. Chem. Soc., Dalton Trans.* **1999**, 3719.

Table 1. Some ^{13}C NMR Parameters (δ, J(CP)/Hz) for Fc′{C≡CRu(PP)Cp′}$_2$ Fragments[a]

complex	dppm/dppe	Fe−C_5H_4	Fe−Cp	Fe−C_{ipso}	Ru−Cp/Cp*	Ph
1-Ru[b]		66.98, 70.46	69.83	77.25	85.94t (2.0)	127.8−140.7
1-Os[b]		66.90, 70.74	69.84	77.81	81.99 (Os)	127.8−140.7
2[c]	50.65t (21.4)	66.24, 70.21	66.27	76.42	80.45	129.6−140.1
3-Ru[b]	28.72−29.34	66.75, 70.31	69.69	76.79	83.18t (2.3)	128.2−144.3
3-Os[b]	30.05−30.67	66.66, 70.69	69.72	77.42	78.62t (2.3)	126.6−143.9
4[b]	29.91−30.53	66.81, 70.19	69.69	77.77	10.77, 92.91	127.8−140.4
10[d]	29.90−30.51	65.21, 71.52, 71.84, 73.43	69.83	79.01	10.76, 92.97	127.9−140.4
11		65.00, 68.64, 71.14, 71.45	70.95	81.37	91.47	128.4−134.4
12	47.06t (22.2)	67.79, 70.66 71.88, 75.15	72.27	74.61	85.09	128.1−140.8
13-Ru	21.46−22.08, 26.69−27.25	68.10, 70.57, 71.62, 72.42, 75.19	72.23	75.44	86.75	127.0−142.5
13-Os	22.78−23.50, 28.93−29.75	68.19, 70.91, 71.84, 75.29	72.45	75.36	83.96 (Os)	125.4−143.4
14	23.85−24.52, 25.21−25.89	68.20, 70.25, 70.38, 71.39	71.09	76.33	8.35, 98.19	128.3−137.3
15		65.91, 72.36, 73.03, 75.60		77.21	91.76	128.5−134.4
16		67.92, 72.36, 73.03, 75.56		77.21	91.82	128.5−134.4
17		67.09, 69.84		77.20	93.84	125.4−136.4, 163.3−165.3
18	26.84−27.48	65.41, 69.56		78.01	90.93	125.4−136.3, 163.2−165.1
19	28.13−29.67	66.24, 68.55		80.02	9.87, 80.02	125.3−136.3, 163.3−165.3

[a] $CDCl_3$ unless otherwise stated. [b] C_6D_6. [c] d_8-Toluene. [d] $SiMe_3$ δ 0.91.

Table 2. ^{13}C NMR Parameters (δ, J(CP)/Hz) for Ethynyl, Dienyl, and Vinylidene Ligands[a]

Alkynyls

	C(1)	C(2)
1-Ru[b]	106.26t (25.7)	109.20
1-Os[b]	82.74t (17.8)	104.13
2[c]	105.76t (25.8)	107.39t (17.5)
3-Ru[b]	106.76t (26.4)	107.29
3-Os[b]	83.41t (18.6)	102.15
4[b]	119.79t (25.2)	104.50
10 tcne adducts	103.76, 122.12t (25.2)	90.34, 106.86

	C(1)	other dienyl	CN
11	217.87d (13.3)	67.48, 84.13d (8.4), 91.50	111.84, 115.94, 119.52d (7.6), 120.05
12	189.12	70.26, 82.87, 91.64	113.33, 115.34, 115.42, 119.85
13-Ru	186.67d (4.0)	72.42, 75.44, 85.53	113.51, 114.59, 115.22, 119.92
13-Os	188.62m, 197.68m	93.61t (2.6)	114.36, 115.99, 116.43, 121.90
14	222.58d (12.9)	66.71, 79.58d (6.9), 98.35	112.32d (2.6), 118.00d (1.2), 119.58d (1.8)
15	216.28d (13.1)	26.86, 65.37d (3.0), 83.46, 84.99d (8.3)	111.58d (2.5), 115.58, 119.38d (7.4), 119.60
16	217.20d (13.1)	26.97, 65.30d (2.6), 83.71, 84.50d (8.6)	111.93d, (2.6) 115.55, 119.45d (7.4), 119.60

Vinylidenes

	C(1)	C(2)	Me
17	354.56t (16.0)	119.41, 121.58	12.06
18	353.89t (17.3)	99.96, 119.20, 121.64	9.10
19	349.61t (17.2)	102.66, 116.46	9.87

[a] $CDCl_3$ unless otherwise stated. [b] C_6D_6. [c] d_8-Toluene.

Scheme 2

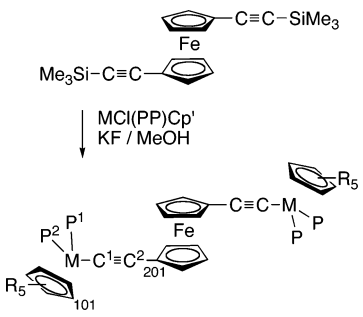

	M	PP	R
5	Ru	$(PPh_3)_2$	H
6	Ru	dppe	H
7	Ru	dppe	Me
8	Fe	dppe	Me

system upon oxidation. The ES-MS contains a weak M^+ at m/z 1614. No NMR spectra of [**5**]PF_6 could be obtained as a result of the paramagnetic nature of this compound.

Electron-deficient alkenes, such as tetracyanoethene (tcne), readily add to C≡C triple bonds adjacent to transition metals to give tetracyano-cyclobutenyl or -butadienyl complexes, or allylic (vinylcarbene) complexes, according to conditions (Scheme 3).[11−13] Alkynylferrocenes have recently been shown to undergo similar reactions to give the corresponding *s-cis*-butadienyl derivatives.[14] Reactions between tcne and either **1** or **4** proceeded readily to give the allylic complexes

(11) Davison, A.; Solar, J. P. *J. Organomet. Chem.* **1979**, *C13*, 166.
(12) (a) Bruce, M. I.; Hambley, T. W.; Snow, M. R.; Swincer, A. G. *Organometallics* **1985**, *4*, 494. (b) Bruce, M. I.; Hambley, T. W.; Snow, M. R.; Swincer, A. G. *Organometallics* **1985**, *4*, 500. (c) Bruce, M. I.; Hambley, T. W.; Liddell, M. J.; Swincer, A. G.; Tiekink, E. R. T. *Organometallics* **1990**, *9*, 2886. (d) Bruce, M. I.; Low, P. J.; Skelton, B. W.; White, A. H. *New J. Chem.* **1998**, *22*, 419.
(13) Onitsuka, K.; Ose, N.; Ozawa, F.; Takahashi, S. *J. Organomet. Chem.* **1999**, *578*, 169.
(14) Mochida, T.; Yamazaki, S. *J. Chem. Soc., Dalton Trans.* **2002**, 3559.

Scheme 3

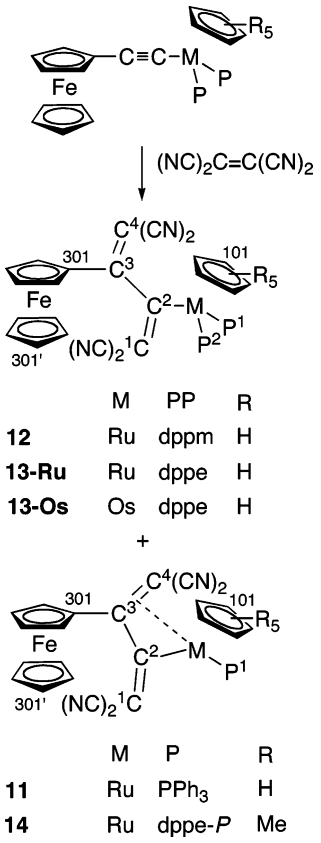

11 and **14**, respectively, whereas similar reactions with **2**, **3-Ru/Os** gave the butadienyls **12**, **13-Ru/Os**.

The dienyl and allylic forms of the tcne adducts could be distinguished by their ^{31}P NMR spectra, which contained resonances at δ 40.74 (PPh_3 in **11**), 7.31 and 8.90 [J(PP) 80.7 Hz, dppm in **12**], 65.32 and 80.09 [J(PP) 56.1 Hz, dppe in **13-Ru**], and −9.95 and 38.64 [J(PP) 29.6 Hz, dppe in **14**]). In the latter, the resonance at δ −9.95 is assigned to the noncoordinated PPh_2 group. In addition, the conformation of the cyanocarbon ligands in these complexes renders the two ^{31}P nuclei in the dppm or dppe ligands inequivalent, and the corresponding resonances are found as AB quartets. In the case of **14**, the opening of the Ru−P−C−C−P chelate ring during the reaction is confirmed by the ^{31}P NMR spectrum, which contains two pseudodoublets (an AB quartet) at δ −10.0 and 38.7, and the X-ray structure (below).

The IR spectra contained one (**11**) or two (**12**, **13-Ru/Os**, **14**) ν(CN) bands at ca. 2200 cm^{-1}, and the ^{1}H spectra contain the resonances expected from the various Cp, substituted C_5H_4, and phosphine ligands. In the ^{13}C NMR spectra of **11**−**14** (Tables 1 and 2), the C_5H_4 ring carbons appear as four signals between δ 65 and 76 as a result of the asymmetry of the cyanocarbon substituent. The C_{ipso} resonances move downfield from the alkynyl precursors to δ ca. 84−87 for the η^1-dienyl compounds and to δ ca. 91−92 for the allylic systems. Fe−Cp, Ru−Cp, and Os−Cp singlets occur at δ ca. 70−72, 84−87, and 84, respectively, while the Cp* ligand in **14** gives rise to signals at δ 8.35 (Me) and 98.2 (ring C). Resonances for the CN groups appear in the region δ_C 111−120, some resonances showing a doublet coupling to phosphorus and tentatively assigned to the CN

Scheme 4

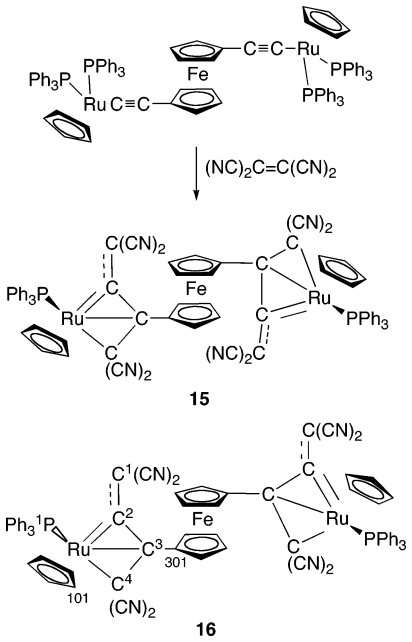

groups attached to C_α. The skeletal carbons of the allylic ligand resonate at δ_C ca. 65−67, 80−85, 85−91, and 218−223; the strong downfield shift of the latter is consistent with the presence of multiple-bond character in the Ru−C(2) bond revealed by the X-ray structure. In the η^1-dienyl complexes **12** and **13**, a resonance at δ ca. 187−190 is also assigned to C(2), being deshielded by both the electron-rich metal center and the electron-withdrawing $=C(CN)_2$ group. Atom C(3) resonates at δ ca. 91−93, while the other skeletal carbons of the dienyl group are found between δ ca. 70 and 75. The ES mass spectra were generally obtained from solutions containing NaOMe, used to enhance ionization,[15] and contained the ions $[M + Na]^+$ or, in the case of **12** and **14**, $[2M + Na]^+$.

Further characterization was achieved from X-ray structural determinations for **11**, **13-Ru/Os**, and **14**, the latter confirming the presence of the monodentate dppe-*P* ligand. Also revealed was the presence of an "impurity" that cocrystallized with **14** with essentially the same structure, but with an oxygen attached to P(2). While we were not able to assign a ν(PO) band in the IR spectrum of **14** with any confidence, re-examination of the crystallographic sample by ^{31}P NMR spectroscopy revealed the presence of a second resonance at δ 34.30 [J(PP) 28.7 Hz], assigned to the P=O group.

The reaction between **5** and 2 equiv of tcne afforded an inseparable diastereomeric mixture of two conformers (**15** and **16**) of the allylic complex (Scheme 4). After heating the mixture in refluxing benzene for 2 days, isomerization of **15** occurred to give exclusively **16**. Confirmation of the structure proposed on the basis of elemental microanalyses and their ^{1}H NMR spectra (only one PPh_3 ligand present) was obtained by a single-crystal X-ray structural determination of **16**. The two diastereomers differ in the relative stereochemistries about the two Ru centers. For **16**, both CN groups of the $=C(CN)_2$ group are on the same face, whereas for

(15) Henderson, W.; McIndoe, J. S.; Nicholson, B. K.; Dyson, P. J. *J. Chem. Soc., Dalton Trans.* **1998**, 519.

Scheme 5

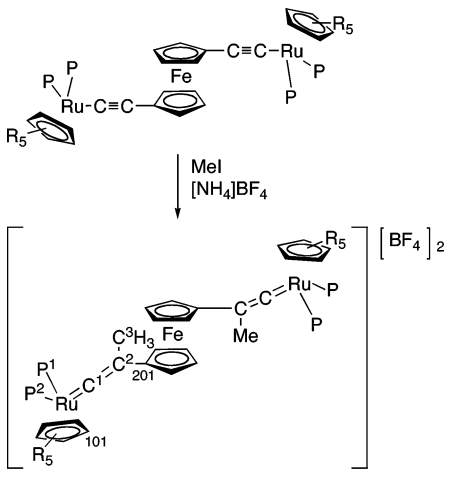

	PP	R
17	$(PPh_3)_2$	H
18	dppe	H
19	dppe	Me

15, they are on opposite faces. As remarked upon earlier, the Ru−C(2) separation is short [1.981(7) Å], suggesting a degree of multiple-bond character, which can be interpreted as giving some carbenic character to this carbon atom.

Addition of electron-deficient alkenes such as tcne to alkynyl−transition metal compounds proceeds via a short-lived radical species (which was not observed in the reactions described on this occasion) to give initially a cyclobutenyl complex, which undergoes ring-opening to form the butadienyl derivative (Scheme 3).[12] Similar reactions have been reported recently for HC≡CFc, FcC≡CFc, and FcC≡CC≡CFc.[14] If the metal center contains easily displaceable ligands, further attachment of the dienyl ligand by formation of a η^3-ligand with concomitant loss of a two-electron donor ligand may then occur. Here, we find the reaction stopping at the dienyl stage for **12**, **13-Ru**, and **13-Os**, which contain chelating dppm or dppe ligands, but proceeding to the η^3-dienyl for **11** (containing monodentate PPh_3) and, surprisingly, also for **14**, in which the original η^2-dppe ligand becomes monodentate. No doubt this is the result of the increased steric hindrance of Cp* compared with Cp.

Another common reaction of alkynyl groups attached to electron-rich transition metal centers is the addition of cationic electrophiles, such as the proton or Me^+, to give the corresponding vinylidenes.[16] Reactions between **5**, **6**, and **7** and MeI were carried out in thf in the presence of $Na[BPh_4]$ to give dark red [1,1′-{Cp′(PP)Ru(=C=CMe)}$_2$Fc′][BPh_4]$_2$ [Cp′ = Cp, PP = $(PPh_3)_2$ (**17**), dppe (**18**); Cp′ = Cp*, PP = dppe (**19**)] (Scheme 5). These derivatives were readily identified by the large downfield shifts found for the Ru=*C*=C carbons at δ ca. 350−355, showing a triplet J(CP) of ca. 17 Hz, characteristic of a vinylidene carbon. Other resonances were as expected, with C_β at δ ca. 120 and the Me signals at δ 9−12. The IR spectrum contains ν(CC) bands at 1650 and 1579 cm^{-1}. The ES mass spectra contained ions assigned to the parent dications.

(16) (a) Bruce, M. I.; Swincer, A. G. *Adv. Organomet. Chem.* **1983**, *22*, 59. (b) Bruce, M. I. *Chem. Rev.* **1991**, *91*, 197.

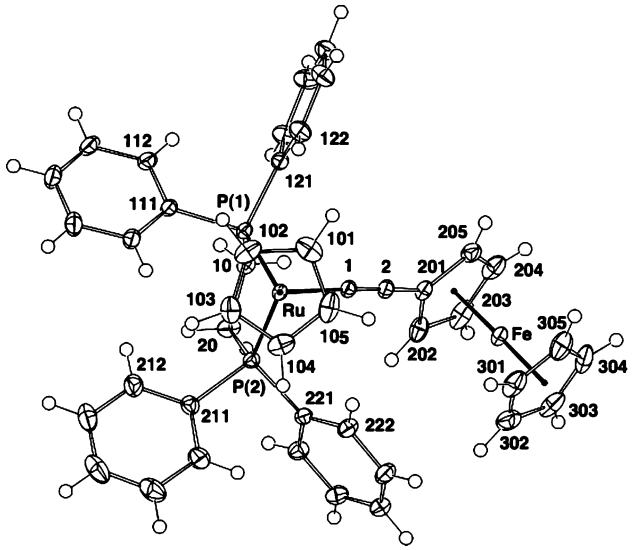

Figure 1. Projection of a molecule of Ru(C≡CFc)(dppe)-Cp (**3-Ru**).

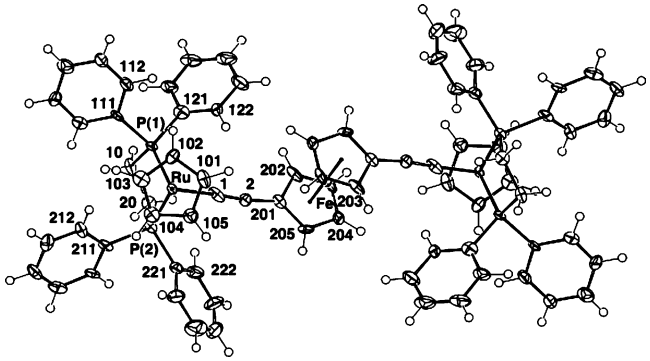

Figure 2. Projection of a molecule of 1,1′-{Cp(dppe)RuC≡C}$_2$Fc′ (**6**).

Molecular Structures. The structures of the alkynyl complexes **1**−**4**, **6**, **7**, and **8** have been determined by crystallographic methods. Plots of molecules of **3-Ru** and **6**, which are representative, are given in Figures 1 and 2, and selected bond distances and angles from the entire series are collected in Table 3. Geometries of the M(PP)Cp′ fragments are similar to those of many previously reported examples, the structural determinations of **7** and **8** allowing comparison of the appropriate parameters that involve the metal atoms, the iron being included in square brackets. The Ru−P distances range between 2.246(4) and 2.2864(7) Å [2.179, 2.185(3) Å], the average Ru−C(Cp) distances fall between 2.23 and 2.25 Å [2.13 Å], and Fe−C_5 ring distances within the ferrocenyl moieties range between 2.03 and 2.05 Å [2.06 Å]. All complexes have pseudo-octahedral geometries about the metal centers, with P(1)−M−P(2) angles reflecting the bite angles of the tertiary phosphines, e.g., PPh_3, 100.97°, 83.96(11)°, dppm, 71.30(3)°, dppe ca. 83° [85.86(9)° for Fe]. Angles P(1,2)−Ru−C(1) range between 80.6° and 90.7(4)°, there being surprisingly little difference between those in **7** and **8** [range 84.0−86.7-(3)°]. The disubstituted ferrocenes are centrosymmetric and isostructural.

Distances involving the alkynyl ligands are also within previously observed ranges, e.g., M−C(1) between 2.00(1) and 2.023(1) Å [1.913(9) Å for Fe], C(1)−C(2) 1.206(4)−1.25(2) Å [1.23(1) Å for **8**], and C(2)−

Table 3. Selected Bond Distances and Angles for 1-Ru/Os, 2–4, and 6–8

	1-Ru	1-Os[a]	2	3	4	6	7	8[b]
				Bond Distances (Å)				
Ru–P(1)	2.2864(7)	2.287(1)	2.2585(8)	2.2460(4)	2.2482(7)	2.259(3)	2.268(1)	2.185(3)
Ru–P(2)	2.2850(7)	2.289(1)	2.2572(7)	2.2563(4)	2.2746(7)	2.254(3)	2.260(1)	2.179(2)
Ru–C(cp)[c]	2.219–2.257(3)	2.218–2.257(5)	2.239–2.252(3)	2.236–2.256(2)	2.221–2.266(3)	2.23–2.27(1)	2.225–2.261(3)	2.092–2.147(8)
(av)	2.234(16)	2.233(16)	2.246(5)	2.246(8)	2.248(18)	2.246(15)	2.248(16)	2.127(21)
Fe–C(cp)	2.024–2.079(3)	2.026–2.085(5)	2.037–2.076(4)	2.027–2.080(1),	2.031–2.058(3)	2.02–2.07(1)	2.039–2.076(5)	2.050–2.084(9)
Fe–C(cp′)	2.023–2.045(4)	2.018–2.036(6)	2.041–2.047(4)	2.028–2.049(2)	2.026–2.038(3)	[2.02–2.07(1)]	[2.039–2.076(5)]	[2.050–2.084(9)]
primed (av)	2.045(20)	2.045(24)	2.049(16)	2.044(22)	2.040(13)	2.05(2)	2.053(14)	2.062(16)
unprimed (av)	2.035(8)	2.029(7)	2.044(2)	2.039(9)	2.033(4)	[2.05(2)]	[2.053(14)]	[2.062(16)]
Ru–C(10)	1.88_0	1.87_6	1.89_6	1.89_5	1.88_4	1.89_2	1.89_7	1.75_0
Fe–C(20, 20′)	1.65_7, 1.65_4	1.63_9, 1.63_7	1.64_6, 1.64_7	1.63_8, 1.65_3	1.64_2, 1.64_2	1.64_8 [1.64_8]	1.65_2 [1.65_2]	1.66_5 [1.66_5]
Fe–C(201)	2.079(3)	2.085(4)	2.076(3)	2.080(1)	2.058(2)	2.07(1)	2.076(4)	2.084(9)
Ru–C(1)	2.017(3)	2.026(4)	2.005(3)	2.023(1)	2.013(2)	2.00(1)	2.015(3)	1.913(9)
C(1)–C(2)	1.217(4)	1.212(4)	1.220(4)	1.219(2)	1.206(4)	1.25(2)	1.210(4)	1.23(1)
C(2)–C(201)	1.432(4)	1.425(6)	1.425(5)	1.431(2)	1.431(4)	1.43(2)	1.440(5)	1.45(1)
				Bond Angles (deg)				
P(1)–Ru–P(2)	100.97(3)	100.61(4)	71.30(3)	83.95(1)	83.46(2)	83.96(11)	83.27(4)	85.86(9)
P(1)–Ru–C(1)	87.38(8)	87.9(1)	81.76(9)	81.14(4)	80.60(7)	90.7(4)	85.2(1)	86.7(3)
P(2)–Ru–C(1)	90.62(8)	90.6(1)	84.71(8)	81.70(4)	88.05(7)	80.6(3)	84.0(1)	84.9(2)
P(1)–Ru–C(10)	122.$_8$	122.$_2$	138.$_7$	132.$_8$	134.$_4$	128.$_5$	134.$_4$	133.$_4$
P(2)–Ru–C(10)	123.$_3$	123.$_9$	135.$_4$	130.$_7$	132.$_7$	134.$_0$	132.$_9$	131.$_3$
C(1)–Ru–C(10)	122.$_6$	122.$_5$	124.$_2$	128.$_0$	120.$_2$	123.$_4$	119.$_8$	118.$_8$
C(20)–Fe–C(20′)	177.$_9$	178.$_4$	178.$_7$	178.$_9$	177.$_3$	180	180	180
Ru–C(1)–C(2)	175.6(2)	175.2(3)	178.7(3)	173.3(1)	177.0(2)	176(1)	175.2(4)	173.2(7)
C(1)–C(2)–C(201)	174.2(3)	173.9(4)	171.3(3)	172.4(1)	177.6(2)	173(1)	176.6(5)	178.8(7)

[a] For Ru, read Os. [b] For Ru, read Fe. [c] C(n0) are the Cp centroids.

Figure 3. Projection of a molecule of Ru{C[=C(CN)$_2$]CFc=C(CN)$_2$}(dppe)Cp (**13-Ru**).

Figure 4. Projection of a molecule of Fc′[{η^3-C[C(CN)$_2$]C=C(CN)$_2$}Ru(PPh$_3$)Cp]$_2$ (**16**).

C(201) 1.425(5)–1.45(1) Å. Of some interest is the Fe–C(201) ring–metal distance, which is often the longest of the 10 C(ring)–Fe distances in each molecule, probably because of weakening of the ring–Fe bond as a result of electron removal by the substituent. As anticipated, the Ru–C(1)–C(2)–C(201) arrays are essentially linear, the maximum deviation being found at C(2) in **2** [171.3(3)°]. However, as others have pointed out in a recent extensive survey,[17] factors involving bending at the carbon atoms of alkyne and poly-yne chains are not well understood, most discussions concluding that crystal-packing effects resulting from low bending modes at the chain carbons are the most likely cause.

The tcne adducts **11**, **13-Ru**, **13-Os**, **14**, **16**, and **19** were also crystallographically characterized, and representative molecular plots of **13-Ru**, **16**, and **19** are shown in Figures 3–5, with selected bond parameters given in Table 4. In **13-Ru/Os**, the σ-dienyl structure of the cyanocarbon ligand is confirmed, with Ru–C(2) 2.086(2) Å. Here, the Ru–P(1,2) separations [2.3328, 2.3054(6) Å] are somewhat longer than those found in the parent alkynyls, probably because the back-bonding into the tertiary phosphine is reduced as a result of the strongly electron-withdrawing nature of the cyanocar-

(17) Szafert, S.; Gladysz, J. A. *Chem. Rev.* **2003**, *103*, 4175.

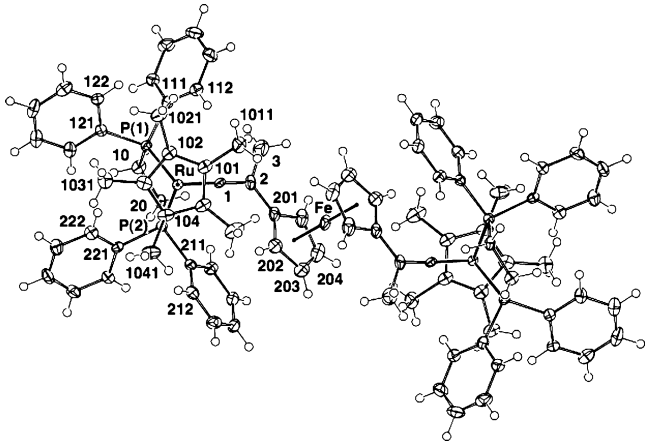

Figure 5. Projection of the cation in [Fc′{CMe=C=[Ru(dppe)Cp*]}$_2$](BPh$_4$)$_2$ (**19**).

bon ligand. Within the latter, the distinction between C−C single [C(1)−C(2) 1.491(3)/1.495(5) Å; values for Ru/Os] and C=C double bonds [C(1)−C(110) 1.380(3)/1.390(5) Å; C(2)−C(210) 1.362(3)/1.372(5) Å] is clear, with the Fc substituent linked by C(301)−C(3) [1.461(3)/1.459(5) Å].

The so-called allylic complexes Ru{η^3-C(CN)$_2$CFcC=C(CN)$_2$}(P)Cp (P = PPh$_3$ **11**, dppe-*P* **14**) and the disubstituted derivative Fc′[{η^3-C[C(CN)$_2$]C=C(CN)$_2$}Ru(PPh$_3$)Cp]$_2$, **16**, contain the cyanocarbon ligand acting as a three-electron donor to the ruthenium center. Examples of this type of complex have been reported before, there being some discussion as to the nature of the bonding of this ligand. The short Ru−C(2) distances [1.978−1.982(3) Å] are consistent with a degree of multiple bonding, which is also reflected in the ^{13}C chemical shifts of these carbons (δ ca. 180). The separations Ru−C(3) and Ru−C(4) are between 2.123 and 2.171(3) and 2.199 and 2.217(3) Å, respectively, which are consistent with an olefinic η^2 interaction. The C(2)−C(3) and C(3)−C(4) separations suggest a degree of delocalization, although the C(1)−C(2) separations are short [1.34−1.363(4) Å] and are also consistent with a C=C double bond. The best interpretation is probably as a chelating vinyl carbene, as found earlier.[12]

Of interest in the structure of **14** is the partial occupancy of an oxygen atom attached to P(2) [P(2)−O(2) 1.24(1) Å, C(02)−P(2)−O(2) 118.8(6)°] and supported by the presence of a second resonance in the ^{31}P NMR spectrum. It is likely that during workup partial oxidation of the free P(2) atom in **14** occurred. On an earlier occasion, we described the formation of a monodentate dppe complex, accompanied by the analogous dppeO derivative, although in that instance, separation and full characterization of the two compounds was possible.[18]

The bis-vinylidene complex **19** is centrosymmetric, and the structure confirms the site of addition of the Me group. The Ru−P distances [2.298, 2.319(1) Å] are longer than those found in neutral complexes, as a result of removal of charge to the positive center. The Ru−C(1) [1.859(4) Å] and the C(1)−C(2) distances [1.331(6) Å] confirm the vinylidene formulation, with considerable shortening and lengthening, respectively, when compared with the precursor **7**. Other parameters are similar to those found in related complexes, such as [Ru(=C=CMePh)(PPh$_3$)$_2$Cp]I.[19]

Ruthenium−Osmium Pairs. The structure determinations for the ruthenium/osmium pairs **1-Ru/Os** and **13-Ru/Os** allow a comparison of structural parameters involving the two metals. The two sets of complexes are each isomorphous, with differences in unit cell volume only 6 (**1**) or −14 Å^3 (**13**). As expected from previous results, bond lengths (Å) involving the two metals are essentially identical: M−P 2.286(1)/2.287(1) for **1**, 2.3054, 2.3328(6)/2.2978(9), 2.3278(9) for **13**; M−C(Cp) (av) 2.234(16)/2.233(16) for **1**, 2.245(6)/2.255(7) for **13**, M−C(1) 2.017(3)/2.026(4) for **1**; M−C(2) 2.086(2)/2.065(3) for **13**.

Electrochemistry. The electrochemical responses of complexes **1-Ru**, **3-Ru**, and **4**, together with the corresponding trimetallic complexes [**5**]PF$_6$, **6**, and **7**, were examined by cyclic voltammetry. All potentials were referenced against internal ferrocene/ferrocinium or colbatocene/cobaltocenium standards and converted to the saturated calomel electrode (SCE) scale.[20] At a scan rate $v \geq 100$ mV s^{-1}, each complex displayed two chemically reversible oxidation processes at moderate potentials, which were separated by 530−690 mV (Table 5). The equal current ratios and peak areas, and hence number of electrons transferred during each oxidation event, indicate each wave to be associated with a one-electron redox process. In the case of the trimetallic species this clearly points to substantial interactions between the metal centers, which decouple the oxidation potentials of the otherwise identical ruthenium centers. A third oxidation process could also be detected nearer the electrochemical limit of the solvent window. However, the trications generated as a consequence of this third oxidation event were chemically unstable on the time scale of the voltammetry experiment, as evidenced by the observation of a large number of product waves in the reverse cathodic sweep.

It is interesting to note that the first oxidation of the bimetallic complexes (Table 5) occurs at significantly less positive potentials than those of the monometallic models Ru(C≡CPh)(PPh$_3$)$_2$Cp (0.535 V), Ru(C≡CPh)(dppe)Cp* (0.245 V), or ferrocene (0.46 V) collected under identical conditions,[21] probably as a result of the electron-withdrawing effect of the Ph groups. The first oxidation of the trimetallic complexes **5** and **6** was shifted by ca. −170 mV relative to the first oxidation of **1-Ru** and **3-Ru**; the second oxidation processes of the trimetallic complexes were shifted by ca. −230 mV relative to the appropriate bimetallic analogues. Curiously, the first and second oxidation potentials of the Ru(dppe)Cp* derivative **7** are similar to those of **4**. Nevertheless the large separation of the redox potentials in both the bi- and trimetallic complexes indicates the high thermodynamic stabilities of the monocations with respect to disproportionation, and large values of the comproportionation constant K_C (10^8−10^{11}) in each case. No doubt this is a function of the differences in the redox centers involved in these events.

(18) Bruce, M. I.; Skelton, B. W.; White, A. H.; Zaitseva, N. N. *J. Organomet. Chem.* **2002**, *650*, 141.

(19) Bruce, M. I.; Humphrey, M. G.; Snow, M. R.; Tiekink, E. R. T. J. *Organomet. Chem.* **1986**, *314*, 213. For a summary of other Ru/Os-vinylidene structures, see: Puerta, M. C.; Valerga, P. *Coord. Chem. Rev.* **1999**, *193−195*, 977.

(20) Pavlishchuk, V. V.; Addison, A. W. *Inorg. Chim. Acta* **2000**, *298*, 97.

(21) Roberts, R. L.; Hartl, F.; Low, P. J. Unpublished work.

Table 4. Bond Distances and Angles for 11, 13-Ru/Os, 14, 16, and 19

	11	13-Ru	13-Os[a]	14	16	19[b]
			Bond Distances (Å)			
Ru−P(1)	2.3883(6)	2.3328(6)	2.3278(9)	2.4061(9)	2.384(2)	2.319(1)
Ru−P(2)		2.3054(6)	2.2978(9)			2.298(1)
Ru−C(cp)[c]	2.209−2.264(2)	2.247−2.261(2)	2.241−2.273(4)	2.199−2.319(3)	2.167−2.263(8)	2.265−2.327(4)
(av)	2.235(21)	2.254(6)	2.255(7)	2.26(5)	2.21(4)	2.291(23)
Fe−C(cp)	2.026−2.045(3)	2.028−2.048(2)	2.017−2.047(4)	2.028−2.054(4)	2.012−2.062(9)	2.046−2.080(5)
	2.039−2.049(3)	2.034−2.058(3)	2.022−2.058(5)	2.029−2.052(4)	[2.012−2.062(9)]	[2.046−2.080(5)]
unprimed (av)	2.036(7)	2.043(8)	2.033(14)	2.046(11)	2.041(19)	2.055(14)
primed (av)	2.045(4)	2.044(9)	2.044(15)	2.044(9)	[2.041(19)]	[2.055(14)]
Ru−C(10)	1.88_4	1.90_4	1.89_9	1.90_0	1.86_6	1.93_9
Fe−C(30, 30′)	1.63_5, 1.64_3	1.65_0, 1.64_6	1.64_4, 1.64_7	1.65_2, 1.65_3	1.65_3 [1.65_3]	1.66_7 [1.66_7]
Fe−C(301)	2.037(2)	2.048(2)	2.047(4)	2.050(3)	2.050(8)	2.080(5)
Ru−C(2)	1.982(2)	2.086(2)	2.065(3)	1.978(3)	1.981(3)	
Ru−C(3)	2.137(2)			2.171(3)	2.123(8)	
Ru−C(4)	2.199(2)			2.217(3)	2.201(8)	
C(1)−C(2)	1.351(3)	1.380(3)	1.396(5)	1.363(4)	1.34(1)	
C(2)−C(3)	1.439(3)	1.491(3)	1.495(5)	1.431(5)	1.43(1)	1.518(7)
C(3)−C(4)	1.476(3)	1.362(3)	1.372(5)	1.477(4)	1.47(1)	1.331(6)
C(3)−C(301)	1.473(3)	1.461(3)	1.459(5)	1.468(4)	1.47(1)	
C−CN	1.439−1.453(3)	1.438−1.443(3)	1.417−1.433(6)	1.433−1.458(5)	1.43−1.46(1)	
(av)	1.44_5	1.43_9	1.42_8	1.44_7	1.44	
			Bond Angles (deg)			
P(1)−Ru−P(2)		82.56(2)	82.25(3)			82.11(4)
P(1)−Ru−C(2)	94.84(6)	97.49(5)	97.65(9)	91.26(9)	95.6(2)	
P(1)−Ru−C(3)	117.46(6)			112.15(8)	119.2(2)	
P(1)−Ru−C(4)	95.63(6)			91.79(8)	97.9(2)	
P(1)−Ru−C(10)	$118._4$	$125._8$	$125._8$	$120._2$	$116._4$	$127._2$
P(2)−Ru−C(2)		99.59(6)	99.66(9)			
P(2)−Ru−C(10)		$124._2$	$125._0$			$134._3$
C(2)−Ru−C(4)	70.19(8)			69.7(1)	70.3(3)	
C(2)−Ru−C(10)	$131._6$	$118._9$	$118._2$	$133._4$	$133._0$	
C(3)−Ru−C(10)	$124._1$			$127._6$	$124._5$	
C(4)−Ru−C(10)	$132._8$			$134._7$	$131._6$	
C(30)−Fe−C(30′)	$177._5$	$176._7$	$177._0$	$178._1$	$178._5$	180
Ru−C(2)−C(1)	145.3(2)	123.9(2)	124.9(3)	144.1(3)	140.7(6)	
Ru−C(2)−C(3)	75.4(1)	122.4(1)	122.6(2)	77.3(2)	75.1(4)	
C(1)−C(2)−C(3)	137.9(2)	112.8(2)	111.6(3)	137.1(3)	141.2(8)	
C(2)−C(3)−C(4)	111.6(2)	119.3(2)	119.1(3)	111.6(3)	112.4(7)	
C(2)−C(3)−C(301)	122.7(2)	116.9(2)	117.4(3)	123.8(3)	122.4(7)	
C(4)−C(3)−C(301)	124.6(2)	123.8(2)	123.5(3)	124.6(3)	124.9(7)	

[a] For Ru, read Os. [b] For **19** read C(20), C(20′), C(201) for C(30), C(30′), C(301): Ru−C(1) 1.859(4), C(2)−C(201) 1.475(7) Å; P(1, 2)−Ru−C(1) 93.9, 81.9(1), C(1)−Ru−C(10) 123.0, Ru−C(1)−C(2) 177.7(4), C(1)−C(2)−C(201) 123.9(4), C(1)−C(2)−C(3) 119.0(4), C(3)−C(2)−C(201) 117.0(4)°. [c] C(n0) are the Cp centroids.

It was of interest to explore the nature of the interactions occurring between the metal centers in these linear heterobimetallic complexes. The electronic (UV−vis−NIR) and vibrational (IR) spectra of the chemically stable, redox-accessible oxidation states of **1-Ru**, **3-Ru**, and **4**−**7** were obtained using spectro-electrochemical methods. Although each complex in this series gave rise to two redox events that were chemically reversible at room temperature on the time scale of the cyclic voltammetric experiment, the dicationic species proved to be less robust on the longer time scale required for the electrolyses in the spectro-electrochemical cells. Others have commented upon the chemical instability of similar species on previous occasions.[8] Infrared spectra were therefore collected at −20 °C, using a low-volume cell of standard design [22] to minimize the time necessary for the experiment, and hence the opportunity for the dications to degrade. The chemical reversibility of each electrogenerated species was established by the recovery of the spectrum associated with the preceding oxidation state following back-reduction of the sample solution.

Table 5. Electrochemistry of Some Ferrocenylethynyl-Metal Complexes 1−19[a]

compound	E_1/V	E_2/V	ΔE/mV	K_C	E_3/V
1-Ru[b]	+0.13	+0.82	690	3.5×10^{11}	
1-Os	+0.05	+0.69	640	6.7×10^{10}	+1.40 (irrev)
2	+0.13	+0.69	560	3.0×10^{9}	+1.40 (irrev)
3-Ru[b]	+0.14	+0.72	580	8.0×10^{9}	
4[b]	+0.05	+0.68	630	4.6×10^{10}	+1.21 (irrev)
[**5**]$^{+c}$	−0.04	+0.58	620	2.9×10^{10}	+0.93 (irrev)
6	−0.03	+0.50	530	9.5×10^{8}	+0.81 (irrev)
7	0.04	+0.68	640	4.3×10^{10}	+1.29 (irrev)
8	−0.31	−0.13	180	1.1×10^{3}	+0.64
9	+0.08	+0.77	690	4.7×10^{11}	+1.65 (irrev)
10	+0.09	+0.75	660	1.5×10^{11}	
11	−1.05	+0.72			+1.79
12	−1.50	+0.74			+1.11
13	−1.47	+0.74			+1.15
14	−1.43	+0.67			+1.67 (irrev)
16	−1.25	−1.03			+0.93
17	+0.48	+0.92 (irrev)			
18	−1.65	−1.56			+0.89 (irrev)[d]
19	+0.44	+0.89 (irrev)			

[a] All electrochemical experiments were performed in 0.1 M $[NBu_4]PF_6$ in CH_2Cl_2, referenced to $FeCp_2/[FeCp_2]^+ = 0.46$ V or $CoCp_2/[CoCp_2]^+ = -0.87$ V. [b] Electrochemistry on literature compounds, comparative values in ref 8a. [c] As compound **5** was not soluble enough for electrochemical studies, these values were obtained from [**5**]PF_6. [d] A second irreversible oxidation wave was observed at +1.15 V.

(22) (a) Hartl, F.; Luyten, H.; Nieuwenhuis, H. A.; Schoemaker, G. C. *Appl. Spectrosc.* **1994**, *48*, 1522. (b) Mahabiersing, T.; Luyten, H.; Nieuwendam, R.; Hartl, F. *Collect. Czech. Chem. Commun.* **2003**, *68*, 1687.

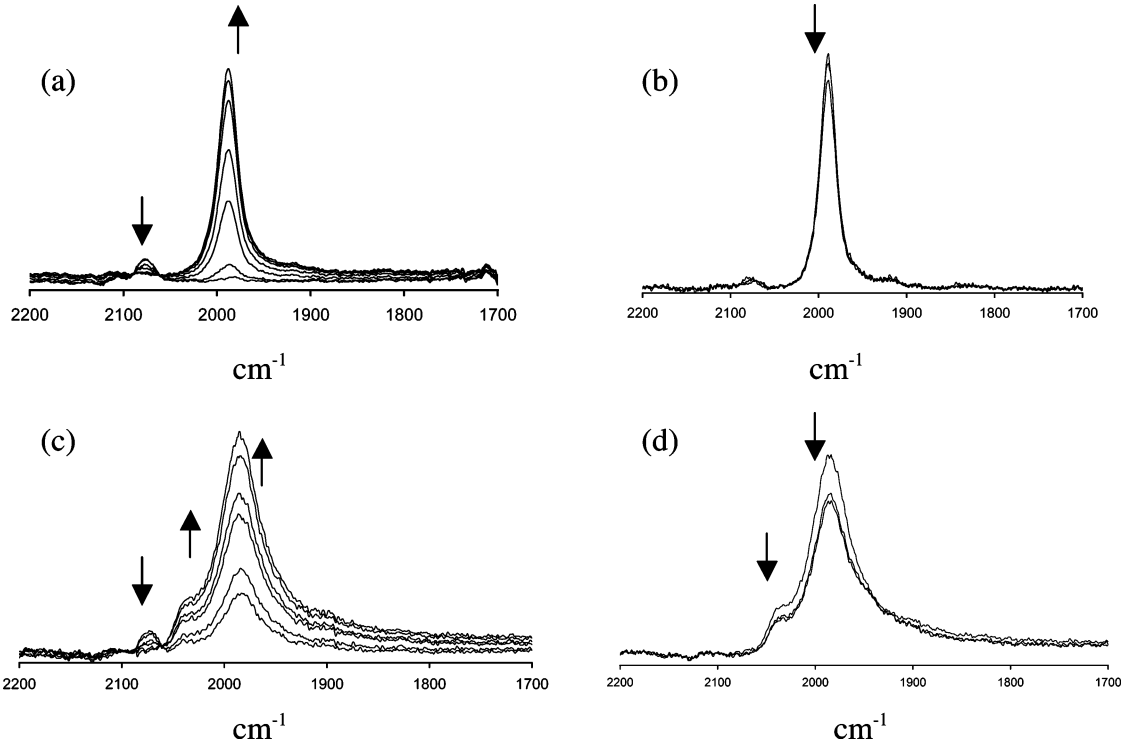

Figure 6. Spectroelectrochemically generated IR spectra of (a) [**1-Ru**]$^{n+}$ (n = 0, 1), (b) [**1-Ru**]$^{n+}$ (n = 1, 2), (c) [**5**]$^{n+}$ (n = 0, 1), and (d) [**5**]$^{n+}$ (n = 1, 2).

Table 6. Infrared ν(CC) Absorptions of Ferrocenylethynyl-Metal Complexes 1-Ru, 3-Ru, and 4-7 in the Oxidation States 0, +1, and +2 (CH_2Cl_2/0.1 M NBu_4PF_6 Solutions)

	ν(CC)/cm^{-1}		
	neutral	+1	+2
1-Ru	2080	1990	1990
3-Ru	2082	1990	1990
4	2080	1984	1984
5	2075	1986, 2039(sh)	1986, 2039(sh)
6	2080	1991, 2043(sh)	1991, 2043(sh)
7	2076	1981, 2037	1981, 2037

In CH_2Cl_2 solution containing 0.1 M $[NBu_4]PF_6$ as supporting electrolyte, each complex in the series **1-Ru**, **3-Ru**, **4**−**7** was characterized by a single, weak ν(C≡C) band at ca. 2080 cm^{-1}. Oxidation of **1-Ru**, **3-Ru**, and **4** to the corresponding monocations resulted in a consistent shift of the ν(C≡C) bands to lower energy ($\Delta\nu \approx$ 90−100 cm^{-1}) (Figure 6, Table 6). The lowering of the ν(C≡C) frequency that occurs upon oxidation may be compared with the corresponding differences in [Ru(C≡CPh)(L_2)Cp′]$^{n+}$ (n = 0, 1; $\Delta\nu \approx$ 150 cm^{-1}).[21] We also note that the absolute values are similar to those of related homometallic iron systems for which delocalized electronic structures have been proposed.[8b] The spectra of the trimetallic species **5**$^+$, **6**$^+$, and **7**$^+$ each exhibited a similarly intense ν(C≡C) band at almost the same energy as the corresponding bimetallic species, in addition to a weak band (or shoulder) near 2040 cm^{-1} (Table 6). In contrast, the second oxidation of the bi- or trimetallic species did not result in a decrease in the ν(C≡C) frequency, but rather in a partial decrease in the intensity of the bands (Figure 6, Table 6). Clearly, while the first oxidation process involves orbitals with some C≡C character, the second must involve an orbital that does not interact with the acetylene moiety. It is therefore likely that the second oxidation event is ferrocene-localized.

The UV−vis−NIR spectra of **1-Ru**, **4**, **5**, and **7** and their one-electron-oxidized products were collected in an optically transparent electrode (OTE) cell (Table 7).[23] The chemically robust neutral and mono-oxidized species could be generated and observed without difficulty at room temperature. However, in spite of the well-behaved CV and IR spectroelectrochemical response, the time required for electrogeneration in the larger volume OTE cell, and possible intrusion of atmospheric moisture, resulted in decomposition of the dioxidized species before reliable spectra could be collected. Cooling the sample to −30 °C did not alleviate the problem.

The electronic absorption spectrum of **1-Ru** was characterized by two bands in the UV region, which tail into a broad ferrocene d−d band near 450 nm/22 000 cm^{-1} (Table 7). The introduction of a second ruthenium acetylide fragment in **5** (electrogenerated in the OTE cell from the soluble sample of [**5**]PF_6]) had little effect on this generalized profile, except for an increase in the intensity of the UV bands relative to the d−d band. One-electron oxidation of **1-Ru** results in subtle shifts in the highest energy bands, accompanied by the appearance of two new bands in the visible region which do not display vibrational fine structure. Similar visible bands are often associated with oxidized (17-e) products derived from group 8 metal alkynyl complexes and are usually attributed to transitions from the occupied orbitals to the stabilized unoccupied orbital set. The delocalized nature of the frontier orbitals can make assignments of such bands difficult, but given the considerable acetylide (π*) character of the LUMO,[24] an MLCT description is a reasonable approximation. In addition, at least two overlapping transitions are clearly

(23) Duff, C. M.; Heath, G. A. *Inorg. Chem.* **1991**, *30*, 2528.

Table 7. Electronic Absorption Spectra of Ferrocenylethynyl-Metal Complexes 1-Ru, 4, 5, and 7 in the Oxidation States 0 and +1

complex	band maxima/cm^{-1} (ϵ/dm^3 mol^{-1} cm^{-1})				
			Neutrals		
1-Ru	35 000 (17400)	28 700 (8550)	~23 000 (2220)		
4	37 600 (22600)	28 500 (9580)			
5					
7	37 900 (26800)	25 800 (14700)	~22 000 (2190)		
			Monocations		
[**1-Ru**]$^+$	33 200 (17582)	23 500 (4656)	17 000 (13270)	6520 (6425)	4760 (49560)
[**4**]$^+$	37 700 (21 589)	30 900 (11 895)	16 100 (6906)	~6470[a]	~5130 (4430)
[**5**]$^+$	33 800 (33 416)	25 100 (8858)	16 400 (15 900)	7360 (5740)	4740 (4130)
[**7**]$^+$	38 610 (26 791)	32 800 (18 711)	16 300 (8997)	6540 (4100)	4590 (4270)

[a] Unresolved.

observed in the NIR region of **1-Ru**. By analogy with Hush-style descriptions of the spectra of mixed valence complexes, these bands are likely due to transitions from lower-lying occupied orbitals to the SOMO.

The spectrum of [**5**]$^+$ displays the same characteristic transitions as observed in the bimetallic analogue **1-Ru**, and it is interesting to note that the lowest energy NIR band is at the same energy in both systems. The availability of samples of [**5**]PF_6 allowed us to record the UV−vis−NIR spectrum of this material in solvents of different dielectric strength free from complications arising from the supporting electrolyte necessary for spectro-electrochemical work. The transitions in [**5**]$^+$ were found to be independent of the solvent environment, which suggests that this monocation is best described with a delocalized electronic structure. The spectra of the more electron-rich complexes [**4**]$^+$ and [**7**]$^+$ were essentially identical to those of their $Ru(PPh_3)_2$-Cp analogues, although the NIR transitions in [**4**]$^+$ were not well resolved (Table 7).

The IR and electronic spectra of the mono-oxidized systems are consistent with an interpretation of the electronic structure, which involves significant delocalization of the odd electron between the ferrocene center and one of the half-sandwich ruthenium centers. The observation of a second ν(C≡C) band in the IR spectra of the trimetallic cations [**5**]$^+$, [**6**]$^+$, and [**7**]$^+$, which is not observed in the bimetallic analogues [**1-Ru**]$^+$, [**3**]$^+$, and [**4**]$^+$, together with the similar electronic absorption spectra of the bi- and trimetallic complexes, suggest that electron exchange between the Ru centers through the Fc center does not occur (i.e., there is no evidence of a new band in the trimetallic species that can be assigned to a photoinduced Ru(II)→Ru(III) MMCT process). The less intense higher-lying shoulder would then be assigned to the largely nonoxidized Ru(C≡C)Cp moiety in the trinuclear cation, which is shifted relative to the neutral precursor by the electron-withdrawing nature of the oxidized fragment. This interpretation is also consistent with the observation of well-separated one-electron anodic waves by cyclic voltammetry.

The second oxidation event, which does not influence the ν(C≡C) frequency, is consistent with a ferrocene-based oxidation process, but unfortunately we have not yet been able to access the two-electron-oxidized complexes either chemically or electrochemically for electronic spectroscopic work.

There are significant waves in the CVs of the cyano-carbon-containing complexes between +0.67 and +0.75 V, and between +0.93 and +1.79 V, which are are tentatively attributed to reversible events at the ferrocene and ruthenium centers. In addition, reversible processes in the region −1.05 to −1.47 V are assigned to reductions of the dicyanomethylene groups on the basis of the well-known ready reduction of tcne to the anion radical and dianion and the proclivity of the cyano-alkene and similar dicyanomethylene compounds to behave as electron acceptors in the formation of molecular complexes with electron-rich systems.[25] Of interest in the CV of the dicationic bis(vinylidene) complex **18** is the presence of two cathodic waves at −1.56 and −1.65 V, assigned to consecutive reduction of the dication and cation, and partially chemically reversible processes at +0.89 and +1.15 V, which we are inclined to assign to oxidation of the ferrocene and ruthenium centers, respectively.

Mössbauer Spectroscopy. The availability of chemically isolable samples of both **5** and [**5**]PF_6 permitted us to investigate the site of oxidation in this complex in more detail using Mössbauer spectroscopy. The spectrum of **5** was recorded at 80 K and contained a unique doublet [IS = 0.539(3) mm s^{-1} vs Fe; QS = 2.357(6) mm s^{-1}] very similar to that of ferrocene itself [90 K: IS 0.531(3) mm s^{-1}; QS 2.419(1) mm s^{-1}].[26] Under similar conditions, the Mössbauer spectrum of [**5**]PF_6 shows a doublet [IS = 0.548(3) mm s^{-1} vs Fe; QS = 0.952(3) mm s^{-1}], which is accompanied by a small doublet with parameters identical with those of **5**, indicating the presence of ca. 10% of the neutral complex in the sample. The observation of a doublet associated with [**5**]PF_6 is not in keeping with the classic Mössbauer spectra of ferrocenium derivatives, which are instead characterized by an almost zero value of the quadrupole splitting.[27] The Mössbauer spectrum of [**5**]PF_6 further supports the concept of a delocalized structure, rather than an oxidation event localized on either the Ru or Fe centers. If one considers complexes [**5**]$^+$, [**6**]$^+$, and [**7**]$^+$ as being derived from the 35-e butadiyndiyl complexes [{Ru(PP)Cp′}$_2$(μ-CCCC)]$^+$,[6] it appears that the introduction of a 1,1′-ferrocenyl moiety within the C_4 bridging ligand hinders delocalization of the unpaired

(24) (a) McGrady, J. E.; Lovell, T.; Stranger, R.; Humphrey, M. G. *Organometallics* **1997**, *16*, 4004. (b) Koentjoro, O. F.; Rousseau R.; Low, P. J. *Organometallics* **2001**, *20*, 4502.

(25) (a) Webster, O. W.; Maher, W.; Benson, R. E. *J. Am. Chem. Soc.* **1962**, *84*, 3678. (b) Ciganek, E.; Linn, W. J.; Webster O. W. In *Chemistry of the Cyano Group*; Patai, S., Ed.; Wiley: New York, 1980; Chapter 9, p 423.

(26) Basta, R.; Wilson, D. R.; Ma, H.; Arif, A. M.; Herber, R. H.; Ernst, R. D. *J. Organomet. Chem.* **2001**, *637−639*, 172.

(27) (a) Collins, R. L. *J. Chem. Phys.* **1965**, *42*, 1072. (b) Nlate, S.; Ruiz, J.; Sartor, V.; Navarro, R.; Blais, J.-C.; Astruc, D. *Chem. Eur. J.* **2000**, *6*, 2544.

electron between the two ruthenium centers. Again it is unfortunate that the instability precluded a Mössbauer investigation of the two-electron-oxidized forms of these materials.

Conclusions

We have described the preparation of several complexes containing electron-rich M(PP)Cp′ (M = Fe, Ru, Os) groups attached to a ferrocene nucleus via one or two C≡C triple bonds. Further reactions with the electrophilic alkene tcne have produced either η^1- or η^3-tetracyanobutadienyl complexes. Crystallographic characterization of the majority of these compounds is described. These compounds were prepared as part of an investigation on the transmission of electronic effects between transition metal end-caps on poly-yndiyl chains containing other redox-active groups interrupting the chain. The combined evidence from UV−vis−NIR and IR spectroelectrochemistry and Mössbauer spectroscopy supports the conclusions that while strong interactions may occur between one Ru(PP)Cp′ moiety and a ferrocenyl center through an ethyndiyl bridge, the ferrocene group acts as an insulator when inserted into the four-carbon chain of the archetypal molecular wires {Ru(PP)Cp′}$_2$(μ-C≡CC≡C).

Experimental Section

General Conditions. All reactions were carried out under dry, high-purity argon using standard Schlenk techniques. Common solvents were dried, distilled under argon, and degassed before use.

Instrumentation. Infrared spectra were obtained on a Bruker IFS28 FT-IR spectrometer. Nujol mull spectra were obtained from samples mounted between NaCl disks. NMR spectra were recorded on Varian 2000 instrument (^{1}H at 300.13 MHz, ^{13}C at 75.47 MHz, ^{31}P at 121.503 MHz). Samples were dissolved in C_6D_6, unless otherwise stated, contained in 5 mm sample tubes. Chemical shifts are given in ppm relative to internal tetramethysilane for ^{1}H and ^{13}C NMR spectra and external H_3PO_4 for ^{31}P NMR spectra. Cyclic voltammograms of complexes **1**, **3**, **4**, [**5**]PF_6, **6**, and **7** were recorded with an EG&G PAR Model 283 potentiostat. The CH_2Cl_2 solutions contained 10^{-3} M complex and 0.1 M $[NBu_4]PF_6$ (Aldrich; recrystallized twice from absolute EtOH and dried overnight under vacuum at 80 °C) as supporting electrolyte. The solutions were placed in an airtight single-compartment three-electrode cell equipped with a Pt disk working electrode (0.42 mm^2 apparent electrode surface, polished with a 0.25 μm diamond paste), Pt gauze auxiliary electrode, and Ag wire pseudo-reference electrode. In the case of **11**−**16**, cyclic voltammograms were recorded using an EG&G PAR Model 263 apparatus with a SCE reference electrode. In all cases, ferrocene or cobaltocence was used as internal calibrant [$E_{1/2}$($FeCp_2$/$[FeCp_2]^+$) = +0.46 V vs SCE in CH_2Cl_2; $E_{1/2}$($CoCp_2$/$[CoCp_2]^+$ = −0.87 V vs SCE in CH_2Cl_2]. The IR spectroelectrochemical experiments at variable temperatures were performed with a previously described OTTLE cell positioned in the sample compartment of a Bio-Rad FTS-7 FT-IR spectrometer.[22] The solutions were 5×10^{-3} M in analyte and 3×10^{-1} M in the supporting electrolyte, $[NBu_4]PF_6$. The UV−vis−NIR spectro-electrochemical measurements were conducted using an OTE cell similar to that described previously,[23] from CH_2Cl_2 solutions containing 1×10^{-1} M $[NBu_4]BF_4$ as supporting electrolyte. Elemental analyses were performed at the Centre for Micro-analytical Services (CMAS), Belmont, Vic.

Reagents. Ferrocene, tetracyanoethene, and $Na[BPh_4]$ (Aldrich) were used as received. The compounds $RuCl(PPh_3)_2Cp$,[28] $FeCl(dppe)Cp^*$,[29] $RuCl(dppe)Cp$,[30] $RuCl(dppe)Cp^*$,[8b] $OsCl(PPh_3)_2Cp$,[31] FcC≡CH,[9] and 1,1′-$(SiMe_3C{\equiv}C)_2Fc$′[9] were prepared using the cited methods.

(a) Ru(C≡CFc)(PPh$_3$)$_2$Cp (1-Ru). A modified literature procedure was employed. $RuCl(PPh_3)_2Cp$ (160 mg, 0.22 mmol), FcC≡CH (78 mg, 0.371 mmol), and $Na[BPh_4]$ (112 mg, 0.318 mmol) were heated in methanol (10 mL) for 1 h at 50 °C. The vessel was cooled in ice, an excess of methanolic sodium methoxide was added, and the mixture was stirred for 15 min. The yellow precipitate that formed was collected on a sinter and washed with methanol and hexane to afford Ru(C≡CFc)$(PPh_3)_2Cp$ (**1**) (140 mg, 71%). Crystals were obtained from benzene−hexane and identified by comparison with the literature.[8a] ^{1}H NMR: δ 4.09, 4.52 (2 × m, 2 × 2H, C_5H_4 of Fc), 4.10 (s, 5H, CpFe), 4.41 (s, 5H, CpRu), 6.97, 7.73 (2 × m, 18 + 12H, Ph). ^{31}P NMR: δ 51.87.

(b) Os(C≡CFc)(PPh$_3$)$_2$Cp (1-Os). Similarly, $OsCl(PPh_3)_2Cp$ (107 mg, 0.131 mmol), HC≡CFc (60 mg, 0.286 mmol), and $Na[BPh_4]$ (111 mg, 0.324 mmol) were heated in refluxing MeOH (10 mL) for 2 h to give Os(C≡CFc)$(PPh_3)_2Cp$ (**1-Os**) (95 mg, 73%). Anal. Calcd ($C_{53}H_{44}FeOsP_2$): C, 64.37; H, 4.48; *M*, 989. Found: C, 64.30; H, 4.51. IR (Nujol): ν(CC) 2069s; other bands at 1640m, 1585w cm^{-1}. ^{1}H NMR: δ 4.11 (br s, 7H, FeCp + C_5H_4), 4.41 (s, 5H, OsCp), 4.51 (m, 2H, C_5H_4), 6.95 (m, 18H, Ph), 7.65 (m, 12H, Ph). ^{31}P NMR: δ 2.93. ES-MS (positive ion, *m/z*): 990, $[M + H]^+$; 781, $[M - HC_2Fc]^+$; 728, $[M - PPh_3]^+$.

(c) Ru(C≡CFc)(dppm)Cp (2). A mixture of RuCl(dppm)Cp (148 mg, 0.253 mmol), HC≡CFc (59 mg, 0.281 mmol), and $Na[BPh_4]$ (105 mg, 0.298 mmol) was heated in a refluxing mixture of thf and NEt_3 (1/1, 20 mL) for 16 h. After removal of solvent, the residue was purified by column chromatography (basic alumina, acetone−hexane, 9/1) to give Ru(C≡CFc)(dppm)Cp (**2**) (105 mg, 55%) as a yellow solid. Crystals were obtained from toluene. Anal. Calcd ($C_{42}H_{36}FeP_2Ru$): 66.41; H, 4.78; *M*, 760. Found: C, 66.50; H, 4.82. IR (Nujol): 2087s, 1586w, 1573w cm^{-1}. ^{1}H NMR (d_8-toluene): δ 3.75 (m, 2H, C_5H_4), 3.80−3.81 (m, 7H, C_5H_4 + CpFe), 4.35−4.60 (m, 2H, CH_2), 4.85 (s, 5H, CpRu), 7.10−7.34 (m, 15H, Ph), 7.87−7.93 (m, 5H, Ph). ^{31}P NMR (d_8-toluene): δ 19.97 (dppm). ES-MS (positive ion, MeOH + NaOMe, *m/z*): 783, $[M + Na]^+$; 760, M^+; 551, $[Ru(dppm)Cp]^+$.

(d) Ru(C≡CFc)(dppe)Cp (3-Ru). As in (a) above, RuCl(dppe)Cp (140 mg, 0.233 mmol), FcC≡CH (75 mg, 0.357 mmol), and $Na[BPh_4]$ (136 mg, 0.386 mmol) were heated at 50 °C in MeOH (15 mL) for 1 h to give Ru(C≡CFc)(dppe)Cp (**3-Ru**) (147 mg, 82%). Orange crystals were obtained from CH_2Cl_2/MeOH and identified by comparison with the literature report.[8a] ^{1}H NMR: δ 2.10−2.30, 2.60−2.80 (2 × m, 2 × 2H, dppe), 3.85, 3.93 (2 × m, 2 × 2H, C_5H_4 of Fc), 3.89 (s 5H, CpFe), 4.72 (s, 5H, CpRu), 6.98, 7.22−7.34, 8.06−8.12 (3 × m, 6 + 10 + 4H, Ph). ^{31}P NMR: δ 87.14.

(e) Os(C≡CFc)(dppe)Cp (3-Os). A mixture of OsCl(dppe)Cp (62 mg, 0.093 mmol), HC≡CFc (32 mg, 0.152 mmol), and $Na[BPh_4]$ (57 mg, 0.167 mmol) was heated in refluxing MeOH (10 mL) for 18 h. After cooling in ice, NaOMe [from Na (5 mg) in MeOH (2 mL)] was added dropwise and the mixture was stirred for 15 min. After this time, solvent was removed under vacuum and the residue was purified by column chromatography (basic alumina, acetone−hexane, 1/9) to give Os(C≡CFc)(dppe)Cp (**3-Os**) (61 mg, 78%) as an orange powder. IR (Nujol): ν(C≡C) 2078s cm^{-1}. ^{1}H NMR: δ 2.23−2.29, 2.51−2.62 (2 × m, 2 × 2H, dppe), 3.85 (br s, 7H, C_5H_4 + Fe−Cp), 3.90 (m, 2H, C_5H_4), 4,62 (s, 5H, Os−Cp), 6.97−8.11 (m, 20H, Ph). ^{31}P NMR: δ 47.24. ES MS (positive ion, MeOH, *m/z*): 864, $[M + H]^+$; 655, $[Os(dppe)Cp]^+$.

(28) Bruce, M. I.; Hameister, C.; Swincer, A. G.; Wallis, R. C. *Inorg. Synth.* **1990**, *28,* 270.
(29) Roger, C.; Hamon, P.; Toupet, L.; Rabaâ, H.; Saillard, J.-Y.; Hamon, J.-R.; Lapinte, C. *Organometallics* **1991**, *10*, 1045.
(30) Alonso, A. G.; Reventos, L. B. *J. Organomet. Chem.* **1998**, *338*, 249.

(f) Ru(C≡CFc)(dppe)Cp* (4). As in (a) above, RuCl(dppe)Cp* (169 mg, 0.245 mmol), HC≡CFc (77 mg, 0.367 mmol), and Na[BPh_4] (102 mg, 0.29 mmol) were heated in refluxing MeOH (15 mL) to give yellow Ru(C≡CFc)(dppe)Cp* (**4**) (165 mg, 75%). Crystals were obtained from acetone. ^{1}H NMR: δ 1.66 (s, 15H, Cp*), 1.80−2.05, 2.60−2.90 (2 × m, 2 × 2H, dppe), 3.98, 4.21 (2 × s, C_5H_4), 4.09 (s, 5H, CpFe), 7.07, 7.24−7.35, 7.94−8.00 (3 × m, 6 + 10 + 4H, Ph). ^{31}P NMR: δ 82.14.

(g) 1,1′-{Cp(Ph$_3$P)$_2$RuC≡C}$_2$Fc′ (5). A mixture of RuCl(PPh$_3$)$_2$Cp (240 mg, 0.331 mmol), 1,1′-($SiMe_3$C≡C)$_2$Fc′ (56 mg, 0.148 mmol), and KF (40 mg, 0.69 mmol) was heated in refluxing thf−MeOH (3/1, 40 mL) for 16 h. The mixture was cooled to rt, and the resulting solution filtered and washed with methanol, ether, and hexane to afford 1,1′-{Cp(Ph$_3$P)$_2$RuC≡C}$_2$Fc′ (**5**) (145 mg, 61%) as a light yellow solid. Anal. Calcd ($C_{96}H_{78}FeP_4Ru_2$): C, 71.46; H, 4.87; *M*, 1614. Found: C, 71.54; H, 4.77. IR (Nujol): ν(C≡C) 2101w, 2069s; other bands at 1654w (br), 1586w, 1573w cm^{-1}. ^{1}H NMR: δ 4.05 (t, *J* 1.8 Hz, 4H, C_5H_4), 4.45 (s, 10H, Cp), 4.58, (t, *J* 1.8 Hz, 4H, C_5H_4), 6.90−7.10 (m, 40H, Ph), 7.73−7.88 (m, 20H, Ph). ^{31}P NMR: δ 52.08. ES-MS (*m/z*): 1614, M$^+$.

(h) 1,1′-{Cp(dppe)RuC≡C}$_2$Fc′ (6). Similarly, from RuCl(dppe)Cp (128 mg, 0.213 mmol), 1,1′-($SiMe_3$C≡C)$_2$Fc′ (40 mg, 0.106 mmol), and KF (13 mg, 0.224 mmol) the complex 1,1′-{Cp(dppe)RuC≡C}$_2$Fc′ (**6**) was obtained (74 mg, 51%) as a light orange solid. Anal. Calcd ($C_{76}H_{66}FeP_4Ru_2$): C, 67.06; H, 4.89; *M*, 1361. Found: C, 67.04; H, 4.90. IR (Nujol): ν(C≡C) 2114w, 2089s; other bands at 1660w (br), 1585w, 1572w cm^{-1}. ^{1}H NMR: δ 2.02−2.22, 2.60−2.88 (2 × m, 2 × 4H, CH_2), 3.57, 3.85 (2 × m, 2 × 4H, C_5H_4), 4.72 (s, 10H, Cp), 6.90−7.02 (m, 12H, Ph), 7.15−7.34 (m, 20H, Ph), 8.05−8.10 (m, 8H, Ph). ^{31}P NMR: δ 87.13. ES-MS (positive ion, *m/z*): 1362, [M + H]$^+$, 98; 682, [M + 2H]$^{2+}$, 100.

In addition 1-(Me_3SiC≡C)-1′-{Cp(dppe)RuC≡C}Fc′ (**9**) (10 mg, 11%) was isolated from the filtrate and purified by column chromatography (basic alumina, 15% acetone−hexane) as an orange-colored solid. Anal. Calcd ($C_{48}H_{46}FeP_2RuSi$): C, 66.28; H, 5.33; *M*, 870. Found: C, 66.30; H, 5.21. IR (Nujol): ν(C≡C) 2146m, 2080s cm^{-1}. ^{1}H NMR: δ 0.23 (s, 9H, $SiMe_3$), 2.10−2.30, 2.60−2.85 (2 × m, 2 × 2H, 2 × CH_2), 3.60−3.61 (m, 2H, C_5H_4), 3.96 (s, 8H, 2 × C_5H_4), 4.69 (s, 5H, RuCp), 6.96−6.98, 7.21−7.31, 8.03−8.08 (3 × m, 20H, Ph). ^{31}P NMR: δ 87.21. ES-MS (*m/z*): 870, M$^+$.

(i) 1,1′-{Cp*(dppe)RuC≡C}$_2$Fc′ (7). Similarly, from RuCl(dppe)Cp* (293 mg, 0.425 mmol), 1,1′-($SiMe_3$C≡C)$_2$Fc′ (66 mg, 0.175 mmol), and KF (21 mg, 36 mmol) in MeOH (60 mL) 1,1′-{Cp*(dppe)RuC≡C}$_2$Fc′ (**7**) (136 mg, 52%) was obtained as an orange solid. Crystals were obtained from thf−2-propanol. Anal. Calcd ($C_{86}H_{86}FeP_4Ru_2$): C, 68.79; H, 5.77; *M*, 1501. Found: C, 68.81; H, 5.63. IR (Nujol): ν(C≡C) 2107w, 2082s; other bands at 1586w, 1572w cm^{-1}. ^{1}H NMR: δ 1.68 (s, 30H, Me), 1.85−2.02, 2.65−2.95 (2 × m, 2 × 4H, CH_2), 4.00, 4.29 (2 × m, 2 × 4H, C_5H_4), 7.00−7.09 (m, 16H, Ph), 7.15−7.28 (m, 12H, Ph), 7.33−7.41 (m, 6H, Ph), 7.97−8.03 (m, 6H, Ph). ^{31}P NMR: δ 82.10. ES-MS (*m/z*): 1501, M$^+$; 752, [M + 2H]$^{2+}$.

(j) 1,1′-{Cp*(dppe)FeC≡C}$_2$Fc′ (8). Similarly, from FeCl(dppe)Cp* (160 mg, 0.256 mmol), 1,1′-($SiMe_3$C≡C)$_2$Fc′ (43 mg, 0.114 mmol), and KF (19 mg, 0.328 mmol) in MeOH (50 mL) 1,1′-{Cp*(dppe)FeC≡C}$_2$Fc′ (**8**) was obtained (9 mg, 6%) as an orange solid. Anal. Calcd ($C_{86}H_{86}Fe_3P_4$): C, 73.20; H, 6.14; *M*, 1411. Found: C, 73.21; H, 6.22. IR (Nujol): ν(C≡C) 2066s cm^{-1}. ^{1}H NMR: δ 1.53 (s, 30H, Me), 1.75−2.00, 2.60−2.90 (2 × m, 2 × 4H, CH_2), 4.14, 4.37 (2 × m, 2 × 4H, C_5H_4), 6.80−7.60 (m, 32H, Ph), 8.00−8.12 (m, 8H, Ph). ^{31}P NMR: δ 101.44. ES-MS (*m/z*): 1411, M$^+$; 706, [M + 2H]$^{2+}$.

(k) 1-(Me_3SiC≡C)-1′-{Cp*(dppe)RuC≡C}Fc′ (10). A mixture of RuCl(dppe)Cp* (197 mg, 0.294 mmol), 1,1′-(Me_3SiC≡C)$_2$Fc′ (106 mg, 0.28 mmol), and KF (17 mg, 0.293 mmol) was heated in refluxing MeOH (40 mL) for 16 h. After cooling, the solid that had separated during the reaction was filtered, washed with MeOH, and dried. Further purification was achieved by dissolving in benzene (50 mL), diluting the filtered solution with hexane (50 mL), and storing in the freezer overnight to afford 1,1′-{Cp*(dppe)RuC≡C}$_2$Fc′ (40 mg, 10%). Removal of solvent from the filtrate afforded pure 1-(Me_3SiC≡C)-1′-{Cp*(dppe)RuC≡C}Fc′ (**10**) (120 mg, 46%) as an orange solid. Anal. Calcd ($C_{53}H_{56}FeP_2RuSi$): C, 67.72; H, 6.00; *M*, 940. Found: C, 67.80; H, 5.97. IR (Nujol): ν(C≡C) 2166w, 2145m, 2106w, 2076s cm^{-1}. ^{1}H NMR: δ 0.27 (s, 9H, $SiMe_3$), 1.63 (s, 15H, C_5Me_5), 1.85−2.10, 2.60−2.90 (2 × m, 2 × 2H, 2 × CH_2), 3.91, 4.08, 4.22, 4.38 (4 × m, 4 × 2H, C_5H_4), 7.06−7.40, 7.93 (m, 20H, Ph). ^{31}P NMR (d_8-toluene): δ 81.90. ES-MS (*m/z*): 941, [M + H]$^+$.

Oxidation of 1,1′-{Cp(Ph$_3$P)$_2$RuC≡C}$_2$Fc′ (5). [$FeCp_2$]PF_6 (33 mg, 0.10 mmol) was added to 1,1′-{Cp(Ph$_3$P)$_2$RuC≡C}$_2$Fc′ (161 mg, 0.10 mmol) in a mixture of CH_2Cl_2 (2 mL) and benzene (15 mL), and the resulting blue solution was stirred at rt for 16 h. After this time, the blue precipitate was collected and washed with Et_2O and hexane to afford [1,1′-{Cp(Ph$_3$P)$_2$RuC≡C}$_2$Fc′]PF_6 ([**5**]PF_6) as a dark blue solid (151 mg, 86%). Anal. Calcd ($C_{96}H_{78}F_6FeP_5Ru_2$): C, 65.57; H, 4.47; *M* (cation), 1614. Found: C, 65.59; H, 4.38. IR (Nujol): ν(CC) 1993s (br), ν(PF) 841s cm^{-1}. ES MS (MeOH, *m/z*): 1614, M$^+$.

Reactions with Tetracyanoethene (tcne). (a) With Ru(C≡CFc)(PPh$_3$)$_2$Cp. A mixture of Ru(C≡CFc)(PPh$_3$)$_2$Cp (58 mg, 0.065 mmol) and tcne (11 mg, 0.086 mmol) was stirred in benzene (10 mL) at rt for 24 h. After removal of solvent, purification of the residue by preparative TLC (dichloromethane) afforded Ru{η^3-C(CN)$_2$CFcC=C(CN)$_2$}(PPh$_3$)Cp (**11**) (37 mg, 75%) as a maroon solid. Crystals were obtained from CH_2Cl_2−hexane. Anal. Calcd ($C_{41}H_{29}FeN_4PRu$): C, 64.32; H, 3.82; N, 7.32; *M*, 766. Found: C, 64.25; H, 3.78; N, 7.25%. IR (Nujol): ν(CN) 2208; other bands at 1609m, 1596m, 1587w, 1571w cm^{-1}. ^{1}H NMR ($CDCl_3$): δ 4.50−4.57 (m, 8H, C_5H_4 + CpFe), 5.39 (m, 1H, C_5H_4), 7.40−7.52 (m, 15H, Ph). ^{31}P NMR ($CDCl_3$): δ 40.74. ES-MS (positive ion, MeOH + NaOMe, *m/z*): 789, [M + Na]$^+$; 766, M$^+$.

(b) With Ru(C≡CFc)(dppm)Cp. Similarly, a mixture of Ru(C≡CFc)(dppm)Cp (60 mg, 0.079 mmol) and tcne (13 mg, 0.10 mmol) in benzene (10 mL) afforded dark red-brown Ru{C[=C(CN)$_2$]=CFc=C(CN)$_2$}(dppm)Cp (**12**) (51 mg, 73%). Anal. Calcd ($C_{48}H_{36}FeN_4P_2Ru$): C, 60.51; H, 3.94; N, 5.76; *M*, 888. Found: C, 61.00; H, 3.72; N, 5.76. IR (Nujol): ν(CN) 2212m, 2199m; other band at 1511m cm^{-1}. ^{1}H NMR ($CDCl_3$): δ 2.46, 3.05, 3.48, 3.89 (4 × m, 4 × 1H, C_5H_4), 4.22 (s, 5H, FeCp), 4.35−4.39 (m, 2H, CH_2), 4.93−5.10 (m, 6H, CH_2 + RuCp), 6.52−6.58, 6.92−6.97, 7.09−7.12, 7.35−7.50, 7.80 (5 × m, 20H, Ph). ^{31}P NMR ($CDCl_3$): δ 8.90 (d, *J* 80.7), 7.31 (d, *J* 80.7). ES-MS (positive ion, MeOH + NaOMe, *m/z*): 1799, [2M + Na]$^+$; 911, [M + Na]$^+$.

(c) With Ru(C≡CFc)(dppe)Cp. To a stirred solution of Ru(C≡CFc)(dppe)Cp (65 mg, 0.084 mmol) in dichloromethane (5 mL) was added tcne (11.5 mg, 0.09 mmol), resulting in a dark red solution. Stirring was continued for 1 h, after which the solvent was removed in vacuo. The residue was purified by chromatography (5% acetone−dichloromethane, flash silica) to give Ru{C[=C(CN)$_2$]=CFc=C(CN)$_2$}(dppe)Cp (**13-Ru**) (56 mg, 74%) as a dark red solid. Crystals were obtained from CH_2Cl_2−hexane. Anal. Calcd ($C_{49}H_{38}FeN_4P_2Ru\cdot0.6CH_2Cl_2$): C, 62.53; H, 4.15; N, 5.88; *M*, 902. Found: C, 62.44; H, 4.18; N, 5.59. IR (Nujol): ν(CN) 2214s, 2204s; also 1508 cm^{-1}. ^{1}H NMR ($CDCl_3$): δ 2.05−2.55 (m, 4H, 2 × CH_2), 3.22, 4.03, 4.47, 4.50 (4 × m, 4 × 1H, C_5H_4), 4.15 (s, 5H, FeCp), 4.97 (s, 5H, RuCp), 6.48−6.54, 7.08−7.20, 7.34−7.40, 7.53−7.57, 7.75−7.81, 7.79−7.95 (6 × m, 20H, Ph). ^{31}P NMR ($CDCl_3$): δ 65.32 (d, *J* 56.1 Hz), 80.09 (d, *J* 56.1 Hz). ES-MS (MeOH + NaOMe, *m/z*): 925, [M + Na]$^+$. Crystals were obtained from CH_2Cl_2−hexane.

(d) With Os(C≡CFc)(dppe)Cp. A mixture of Os(C≡CFc)(dppe)Cp (59 mg, 0.068 mmol) and tcne (11 mg, 0.082 mmol)

Table 8. Crystal Data and Refinement Details

	1-Ru	1-Os	2	3	4	6	7	8
formula	$C_{53}H_{44}FeP_2Ru$	$C_{53}H_{44}FeOsP_2$	$C_{42}H_{36}FeP_2Ru$	$C_{43}H_{38}FeP_2Ru$	$C_{48}H_{48}FeP_2Ru$	$C_{76}H_{66}FeP_4Ru_2 \cdot 2C_6H_6$	$C_{86}H_{86}FeP_4Ru \cdot 2C_4H_8O$	$C_{86}H_{86}Fe_3P_4 \cdot 2C_4H_8O$
MW	899.8	989.0	759.6	773.6	843.8	1517.5	1645.7	1555.3
cryst syst	monoclinic	monoclinic	monoclinic	monoclinic	monoclinic	triclinic	triclinic	triclinic
space group	$P2_1/c$	$P2_1/c$	$P2_1/c$	$P2_1/c$	$P2_1/c$	$P\bar{1}$	$P\bar{1}$	$P\bar{1}$
a, Å	11.489(1)	11.484(1)	13.4266(7)	17.577(2)	19.574(1)	9.918(3)	11.727(1)	10.840(5)
b, Å	16.829(1)	16.822(1)	13.9603(7)	9.573(1)	12.770(1)	10.710(3)	12.127(1)	12.788(5)
c, Å	21.153(2)	21.205(2)	18.912(1)	20.232(2)	16.570(2)	17.525(5)	15.625(1)	15.278(6)
α, deg						89.258(5)	107.713(2)	108.553(7)
β, deg	91.547(7)	91.704(7)	109.370(1)	99.597(3)	109.423(2)	84.795(5)	111.541(2)	95.423(7)
γ, deg						72.660(5)	90.528(2)	95.282(7)
V, Å^3	4089	4095	3344	3357	3906	1769	1950	1982
Z	4	4	4	4	4	1	1	1
D_c, g cm^{-3}	1.46_2	1.60_4	1.50_7	1.53_1	1.43_5	1.42_4	1.40_1	1.30_3
μ, mm^{-1}	0.84	3.6	1.01	0.87	0.87	0.76	0.70	0.67
cryst size, mm	0.38 × 0.26 × 0.04	0.25 × 0.12 × 0.11	0.23 × 0.10 × 0.08	0.38 × 0.16 × 0.09	0.31 × 0.20 × 0.11	0.13 × 0.09 × 0.03	0.31 × 0.15 × 0.07	0.15 × 0.07 × 0.06
$T_{min/max}$	0.88	0.77	0.89	0.86	0.89	0.79	0.59	0.76
$2\theta_{max}$, deg	60	70	60	75	58	50	60	50
N_{tot}	74 939	82 295	54 352	69 672	45 606	16 283	36 052	14 577
N (R_{int})	11 742 (0.069)	17 531 (0.080)	9604 (0.062)	17 633 (0.034)	10 391 (0.042)	6155 (0.096)	11 180 (0.071)	6876 (0.096)
N_o	9088	11 880	7445	13 828	8368	4113	8370	4169
R	0.043	0.045	0.044	0.031	0.034	0.087	0.057	0.079
R_w (n_w)	0.055 (1.5)	0.053 (12)	0.056 (8.5)	0.038 (5)	0.043 (7)	0.114 (70)	0.073 (20)	0.103 (30)

	11	13-Ru	13-Os	14	16	19
formula	$C_{41}H_{29}FeN_4PRu \cdot 0.725CH_2Cl_2$	$C_{49}H_{38}FeN_4P_2Ru \cdot CH_2Cl_2$	$C_{49}H_{38}FeN_4OsP_2 \cdot CH_2Cl_2$	$C_{54}H_{48}FeN_4O_{0.18}P_2Ru \cdot C_3H_6O$	$C_{72}H_{48}FeN_8P_2Ru_2$	$C_{88}H_{92}FeP_4Ru_2^{2+} \cdot 2C_{24}H_{20}B^-$
MW	827.2	986.7	1075.8	1032.9	1345.2	2170.1
cryst syst	monoclinic	monoclinic	monoclinic	monoclinic	monoclinic	monoclinic
space group	$P2_1/c$	$P2_1/n$	$P2_1/n$	$P2_1/n$	$C2/c$	$P2_1/n$
a, Å	16.317(1)	8.9587(6)	8.9577(5)	13.260(2)	15.657(3)	16.267(2)
b, Å	10.2710(8)	19.281(1)	19.265(1)	21.108(3)	14.345(3)	18.328(3)
c, Å	21.581(2)	25.191(2)	25.124(1)	17.984(3)	27.231(5)	18.488(3)
α, deg						
β, deg	101.885(2)	96.774(2)	96.562(1)	104.137(2)	98.409(3)	99.199(3)
γ, deg						
V, Å^3	3539	4321	4307	4881	6050	5441
Z	4	4	4	4	4	2
D_c, g cm^{-3}	1.55_2	1.51_6	1.65_9	1.40_5	1.47_7	1.32_4
μ, mm^{-1}	1.03	0.92	3.52	0.72	0.83	0.52
cryst size, mm	0.48 × 0.22 × 0.18	0.26 × 0.24 × 0.13	0.34 × 0.17 × 0.16	0.15 × 0.15 × 0.07	0.24 × 0.16 × 0.11	0.16 × 0.08 × 0.06
$T_{min/max}$	0.83	0.87	0.68	0.81	0.72	0.87
$2\theta_{max}$, deg	65	75	75	58	53	50
N_{tot}	73 303	89 959	86 300	44 824	28 141	50 761
N (R_{int})	12 512 (0.058)	22 790 (0.043)	22 627 (0.049)	12 194 (0.064)	6165 (0.084)	9526 (0.079)
N_o	9678	16 332	17 452	8885	4409	7044
R	0.042	0.045	0.042	0.047	0.080	0.051
R_w (n_w)	0.054 (14)	0.059 (8)	0.083 (6)	0.060 (20)	0.107 (50)	0.065 (20)

was stirred in benzene (10 mL) at rt for 24 h. After removal of solvent under vacuum, purification of the residue by preparative TLC (acetone−CH_2Cl_2, 2/98) afforded dark red-brown Os{C[=C(CN)$_2$]=CFc=C(CN)$_2$}(dppe)Cp (**13-Os**) (25 mg, 37%). Crystals were obtained from CH_2Cl_2−hexane. Anal. Calcd ($C_{49}H_{38}FeN_4OsP_2\cdot0.5CH_2Cl_2$): C, 57.54; H, 3.80; N, 5.42; *M*, 992. Found: C, 57.58; H, 3.88; N, 4.74. IR (Nujol): ν(CN) 2214s, 2199s; also 1508 cm^{-1}. ^{1}H NMR ($CDCl_3$): δ 2.00−2.50 (m, 4H, CH_2), 2.26, 3.98, 4.49, 5.53 (4 × m, 4 × 1H, C_5H_4), 4.13 (s, 5H, FeCp), 5.03 (s, 5H, OsCp), 6.41−6.47, 7.04−7.14, 7.26−7.58, 7.73, 7.89−7.95 (6 × m, 2 + 3 + 10 + 3 + 2H, Ph). ^{31}P NMR ($CDCl_3$): δ 29.03 (d, *J* 6.8 Hz), 40.79 (d, *J* 6.8 Hz) (AB q). ES-MS (MeOH + NaOMe, *m/z*): 1015, [M + Na]$^+$; 655, [Os(dppe)Cp]$^+$.

(e) With Ru(C≡CFc)(dppe)Cp*. Similarly, a mixture of Ru(C≡CFc)(dppe)Cp* (79 mg, 0.094 mmol) and tcne (14 mg, 0.11 mmol) in benzene (10 mL) gave Ru{η^3-C(CN)$_2$CFcC=C(CN)$_2$}(dppe-*P*)Cp* (**14**) (21 mg, 23%) as a purple solid. Crystals were obtained from acetone−hexane. Anal. Calcd ($C_{54}H_{48}FeN_4P_2Ru$): C, 66.74; H, 4.98; N, 5.76; *M*, 1088. Found: C, 66.86; H, 5.00; N, 5.76. IR (Nujol): ν(CN) 2214m, 2206m; other band at 1588 cm^{-1}. ^{1}H NMR ($CDCl_3$): δ 1.14 (s, 15H, Cp*), 2.35−2.50, 2.52−2.70 (2 × m, 2 × 2H, 2 × CH_2), 4.32, 4.50, 4.53, 5.41 (4 × m, 4 × 1H, C_5H_4), 4.46 (s, 5H, FeCp), 7.30−7.80 (m, 20H, Ph). ^{31}P NMR ($CDCl_3$): δ −9.95 (d, *J* 29.6), 38.64 (d, *J* 29.6). ES-MS (positive ion, MeOH + NaOMe, *m/z*): 2000, [2M + Na]$^+$; 1111, [M + Na]$^+$. As discussed above, the material contained a small amount of the analogous dppeO complex, which gave ^{31}P signals at δ 34.33 (d, *J* 28.7) and 38.64 (d, *J* 28.7).

(f) 1,1′-{Cp(Ph$_3$P)$_2$RuC≡C}$_2$Fc′. A mixture of 1,1′-{Cp(Ph$_3$P)$_2$RuC≡C}$_2$Fc′ (108 mg, 0.067 mmol) and tcne (28 mg, 0.219 mmol) in benzene (10 mL) was stirred for 48 h at rt. After removal of solvent, the residue was purified by preparative TLC (CH_2Cl_2) to give the tcne adduct as a red solid (63 mg, 70%) as a mixture of isomers **15** and **16** (7/3). Anal. Calcd ($C_{72}H_{48}FeN_8P_2Ru_2$): C, 64.29; H, 3.60; N, 8.33. Found: C, 64.18; H, 3.47; N, 8.27. IR (Nujol): ν(CN) 2214s; other band at 1606m (br) cm^{-1}. Major isomer (**15**): ^{1}H NMR: δ 4.52 (s, 10H, RuCp), 4.90, 5.00, 5.11, 5.52 [4 × s (br), 4 × 2H, C_5H_4], 7.39−7.56 (m, 30H, Ph). ^{31}P NMR ($CDCl_3$): δ 40.27. Minor isomer (**16**): ^{1}H NMR ($CDCl_3$): δ 4.53 (s, 10H, RuCp), 4.70, 4.98, 5.24, 5.74 (4 × s, 4 × 2H, C_5H_4), 7.35−7.65 (m, 30H, Ph). ^{31}P NMR ($CDCl_3$): δ 40.29.

After heating complex **15** (35 mg, 0.026 mmol) in refluxing benzene (20 mL) for 2 days, preparative TLC (silica gel, acetone−hexane, 1/1) gave the pure **16** as a light red solid (32 mg, 92%). Crystals were obtained from CH_2Cl_2−hexane. Anal. Calcd ($C_{72}H_{48}FeN_8P_2Ru_2$): C, 64.29; H, 3.60; N, 8.33; *M*, 1346. Found: C, 64.15; H, 3.50; N, 8.38. ES-MS (MeCN, *m/z*): 1364, [M + NH$_4$]$^+$.

Reactions of MeI. (a) With 1,1′-{Cp(Ph$_3$P)$_2$RuC≡C}$_2$Fc′. MeI (10 drops, excess) was added to a suspension of 1,1′-{Cp(Ph$_3$P)$_2$RuC≡C}$_2$Fc′ (55 mg, 0.034 mmol) and Na[BPh$_4$] (55 mg, 0.161 mmol) in thf (10 mL), and the mixture was heated at reflux point overnight. After cooling and removal of solvent, column chromatography (basic alumina, CH_2Cl_2) gave the dark red bis(vinylidene) [1,1′-{Cp(Ph$_3$P)$_2$Ru=C=CMe}$_2$Fc′](BPh$_4$)$_2$ (**17**) (60 mg, 78%). Anal. Calcd ($C_{144}H_{118}B_2FeP_4Ru_2$): C, 76.80; H, 5.28; *M* (cation), 1644. IR (Nujol): 1642s, 1579m cm^{-1}. ^{1}H NMR ($CDCl_3$): δ 1.85 (s, 6H, 2 × Me), 3.93, 4.28 (2 × m, 2 × 4H, C_5H_4), 4.83 (s, 10H, RuCp), 6.86−6.93 (m, 33H, Ph), 7.01−7.06 (m, 17H, Ph), 7.15−7.18 (m, 25H, Ph), 7.35−7.46 (m, 25H, Ph). ^{31}P NMR ($CDCl_3$): δ 42.65. ES-MS (*m/z*): 822, M^{2+}.

(b) With 1,1′-{Cp(dppe)RuC≡C}$_2$Fc′. As in (a) above, MeI (10 drops, excess), 1,1′-{Cp(dppe)RuC≡C}$_2$Fc′ (64 mg, 0.047 mmol), and Na[BPh$_4$] (36 mg, 0.105 mmol) in thf (10 mL) gave the dark red bis(vinylidene) [1,1′-{Cp(dppe)Ru=C=CMe}$_2$Fc′][BPh$_4$]$_2$ (**18**) (60 mg, 63%). Anal. Calcd ($C_{120}H_{112}B_2FeP_4Ru_2$): C, 74.56; H, 5.56: *M* (cation), 1393. Found: C, 74.44; H, 5.60. IR (Nujol): 1650s, 1579m cm^{-1}. ^{1}H NMR ($CDCl_3$): δ 1.13 (s, 6H, 2 × Me), 2.37−2.42 (m, 8H, 4 × CH_2), 3.16, 3.62 (2 × m, 2 × 4H, 2 × C_5H_4), 5.21 (s, 10H, RuCp), 6.81−6.99, 7.20−7.43 (m, 60H, Ph). ^{31}P NMR ($CDCl_3$): δ 78.05. ES-MS (*m/z*): 696.5, M^{2+}.

(c) With 1,1′-{Cp*(dppe)RuC≡C}$_2$Fc′. As in (a) above, MeI (10 drops, excess), 1,1′-{Cp*(dppe)RuC≡C}$_2$Fc′ (40 mg, 0.027 mmol), and Na[BPh$_4$] (31 mg, 0.091 mmol) in thf (10 mL) gave the dark red bis(vinylidene) [1,1′-{Cp*(dppe)Ru=C=CMe}$_2$Fc′][BPh$_4$]$_2$ (**19**) (57 mg, 93%). Anal. Calcd ($C_{134}H_{126}B_2FeP_4Ru_2$): C, 75.21; H, 5.93: *M* (cation), 1532. Found: C, 75.07; H, 5.92. IR (Nujol): 1639s, 1579m cm^{-1}. ^{1}H NMR ($CDCl_3$): δ 1.10 (s, 6H, 2 × Me), 1.42 (s, 30H, Cp*), 2.10−2.60 (m, 8H, 4 × CH_2), 3.13, 3.69 (2 × m, 2 × 4H, 2 × C_5H_4), 6.79−6.94 (m, 15H, Ph), 7.16−7.38 (m, 25H, Ph). ^{31}P NMR ($CDCl_3$): δ 75.89. ES-MS (*m/z*): 766, M^{2+}.

Structure Determinations. Full spheres of diffraction data were measured at ca. 153 K using a Bruker AXS CCD area-detector instrument. N_{tot} reflections were merged to *N* unique (R_{int} quoted) after "empirical"/multiscan absorption correction (proprietary software), N_o with $F > 4\sigma(F)$ being used in the full matrix least squares refinements. All data were measured using monochromatic Mo Kα radiation, $\lambda = 0.71073$ Å. Anisotropic displacement parameter forms were refined for the non-hydrogen atoms, (x, y, z, U_{iso})$_H$ being constrained at estimated values. Conventional residuals R, R_w on $|F|$ are quoted [weights: $(\sigma^2(F) + 0.000n_wF^2)^{-1}$]. Neutral atom complex scattering factors were used; computation used the XTAL 3.7 program system.[32] Pertinent results are given in the figures (which show non-hydrogen atoms with 50% probability amplitude displacement ellipsoids and hydrogen atoms with arbitrary radii of 0.1 Å) and in the Tables 1, 2, and 8. Individual diversions in procedure are noted below as Variata.

Variata. 1, **2**. These compounds are isomorphous and were refined in the same coordinate and cell setting.

7. Isotropic displacement parameter forms were refined for C, O of the solvent molecules, O being assigned here and in **8** on the basis of refinement behavior.

11. Solvent residues were modeled as disordered over a pair of sites with constrained geometries, total occupancy refining to 0.725.

14. A difference map residue in the vicinity of the uncoordinated phosphorus was modeled as a phosphine oxide oxygen impurity fragment, occupancy refining to 0.182(9). Full details of the structure determination (except structure factors) have been deposited with the Cambridge Crystallographic Data Centre as CCDC Nos. 253731−253743, 269428. Copies of this information may be obtained free of charge from The Director, CCDC, 12 Union Road, Cambridge CB2 1EZ, UK (fax: +44 1223 336 033; e-mail: deposit@ccdc.cam.ac.uk or www: http://www.ccdc.cam.ac.uk).

Acknowledgment. We thank the ARC (M.I.B.) and the EPSRC (P.J.L.) for support of this work and Johnson Matthey plc, Reading, for a generous loan of $RuCl_3\cdot nH_2O$. B.G.E. held a Commonwealth Post-graduate Scholarship; R.L.R. holds a postgraduate scholarship from the Durham Chemistry EPSRC Doctoral Training Account. We thank Dr. Azzedine Bousseksou (Toulouse, France) for fruitful discussions concerning the analysis

(31) Bruce, M. I.; Low, P. J.; Skelton, B. W.; Tiekink, E. R. T.; Werth, A.; White, A. H. *Aust. J. Chem.* **1995**, *48*, 1887.

(32) Hall, S. R., de Boulay, D. J., Olthof-Hazekamp R., Eds. *The XTAL 3.7 System*; University of Western Australia: Perth, 2000.

of the Mössbauer spectra and Professor Brian Nicholson (University of Waikato, New Zealand) for the mass spectra. This work was facilitated by travel grants from the Centre National de la Recherche Scientifique (CNRS), the Australian Research Council (ARC IREX and Linkage Exchange programs), and the EU EESD HPMT-CT2001-00311 Marie Curie Training Site (Amsterdam, The Netherlands).

Supporting Information Available: The crystallographic data, in cif format, can be obtained free of charge from the Internet at http://pubs.acs.org.

OM050483L